PLOS ONE

# Crystal structure of penicillin-binding protein 3 (PBP3) from Escherichia coli

--Manuscript Draft--

| | |
|---|---|
| **Manuscript Number:** | PONE-D-14-04293R1 |
| **Article Type:** | Research article |
| **Full Title:** | Crystal structure of penicillin-binding protein 3 (PBP3) from Escherichia coli |
| **Short Title:** | Structure of Escherichia coli PBP3 |
| **Corresponding Author:** | eric sauvage<br>University of Liege<br>Liege, BELGIUM |
| **Keywords:** | cell division; penicillin-binding protein; peptidoglycan; PBP3; ftsI |
| **Abstract:** | In Escherichia coli, penicillin-binding protein 3 (PBP3), also known as FtsI, is a central component of the divisome, catalyzing cross-linking of the cell wall peptidoglycan during cell division. PBP3 is mainly periplasmic, with a 23 residues cytoplasmic tail and a single transmembrane helix. We have solved the crystal structure of a soluble form of PBP3 (PBP357-577) at 2.5 Å revealing the two modules of high molecular weight class B PBPs, a carboxy terminal module exhibiting transpeptidase activity and an amino terminal module of unknown function. To gain additional insight, the PBP3 Val88-Ser165 subdomain (PBP388-165), for which the electron density is poorly defined in the PBP3 crystal, was produced and its structure solved by SAD phasing at 2.1 Å. The structure shows a three dimensional domain swapping with a β-strand of one molecule inserted between two strands of the paired molecule, suggesting a possible role in PBP357-577 dimerization. |
| **Order of Authors:** | eric sauvage |
| | Adeline Derouaux |
| | Claudine Fraipont |
| | Marine Joris |
| | Raphaël Herman |
| | Mathieu Rocaboy |
| | Marie Scloesser |
| | Jacques Dumas |
| | Frédéric Kerff |
| | Martine Nguyen-Distèche |
| | Paulette Charlier |
| **Suggested Reviewers:** | Andrea Dessen<br>Institut de Biologie Structurale Jean-Pierre Ebel, Grenoble, France<br>dessen@ibs.fr<br>A. Dessen is a crystallographer working on penicillin binding proteins |
| | Waldemar Vollmer<br>Professor, Newcastle University<br>waldemar.vollmer@ncl.ac.uk<br>W. Vollmer is an expert of the bacterial cell division. |
| | Sam-Yong Park<br>Professor, Yokohama City University, Japan<br>park@tsurumi.yokohama-cu.ac.jp<br>Professor Park is a crystallographer working on penicillin binding proteins |
| **Opposed Reviewers:** | |
| **Response to Reviewers:** | Dear Editors, |

We have tried to address the concerns of reviewer 1 about the structure. Typographical errors found mainly by reviewer 2 have been corrected and the paper was read by an English native speaker. Finally, as suggested by reviewer 3, we have expanded the description of the structure and modified the figures accordingly. Details follow.

Reviewer #1
1.lines 125-129 … The authors state that PBP3(57-577) crystalization “could not be reproduced despite countless attempts.” First, surely there were not “countless” attempts. About how many attempts were made, and do the authors have any ideas about what the problem might be? This is rather important since it is unlikely that the work can be replicated by others if it cannot be replicated here. Second, with only one successful crystallization, how confident are the authors about the nature of the results?

R: The apparent very narrow range of crystallization conditions resulted in only some very small badly diffracting crystals and one crystal diffracting at 2.5 Å. This sentence was added to the manuscript.
In the case of several PBPs structures, the difficulties encountered in obtaining high resolution x-ray data sets, in reproducing crystals or even obtaining crystals, are mainly due to their nature of multi-domain proteins, for which several relative conformations of the different domains co-exist in solution. That’s why multi-domain protein structures are frequently determined from a single X-ray dataset but this has no impact on the soundness of structure determination.

2. lines 212-213 … The PBP3 structure was evidently not determined de novo, but by comparison with the structure of PBP2 from a different organism, N. gonorrhoeae. This, when combined with the fact that only one crystallization attempt was successful, makes me wonder if this is the real structure of PBP3 or if it is only a single possible structure that can be made to conform to the structure of a somewhat distant homologue. Why can the structure not be generated on its own, and what are the limitations imposed by the modeling method?

R: Structure determination by molecular replacement using the structure of a homologous protein (NgPBP2) is also a standard method that does not impact the confidence that the structure determined corresponds to the protein that has been crystallized. R and Rfree values are good criteria to ensure that the structure corresponds to the X-ray measures, independently of the initial structure used for molecular replacement.
Efforts have been made to clearly show in figure 1 the part of the structure that was determined from X-ray data and the modeled parts of the structure.

3. lines 378-380 … The authors could not reproduce interactions between the PBP3(88-165) fragment and other cell division proteins. If these interactions do not occur, doesn’t this call into question the biological relevance of the structure obtained for this fragment?

R: No. The structure of the domain 88-165 compares well with the equivalent domains of other class B-PBPs. The biological relevance of the swapping associated with the structure of the domain alone is indeed questionable but we think that the discussion states it clearly.

4. In Figure S3, very little of the PBP3(57-577) seems to have co-precipitated with the peptidoglycan preparation. Why? The authors should quantify how much was precipitated and compare it to what might be expected.

R: A similar test was done with LpoA-LpoB (Typas et al, Cell. 2010, 143:1097) without quantification, which is difficult. Clearly, only a fraction of the protein was precipitated. A possible explanation is that PBP3 interacts only with the septal peptidoglycan, which represents only a small proportion of the total peptidoglycan.

Minor comments

5. line 69 … should be “LpoB” (capital “B”)

Done

6. line 256 … should be “PBP-structures” (plural)
OK

Reviewer #2
1.There are many typos and errors in comma usage and grammar that should be corrected.

Minor points:

1. l. 47: it is not clear what is meant by "direct" peptidoglycan synthesis. Is there something like indirect synthesis?
“Direct” has been removed

2. l. 69: should be "LpoB" with capital "B"
Done

3. l. 96: the 2XYT medium should be defined.
Done

4. l. 98: should be "0.5 mM"
Done

5. l. 113/117/119: what is meant with "ch/h" and "cm/h". Flow rates should be given in "ml/min" or "ml/h".

R: Typing error, ch/h doesn’t exist, it’s cm/h (linear flow rate, which is independent of the diameter of the column, instead of the flow rate in ml/h which is dependent of the column diameter). The linear flow rate is preferred by people making a scale-up because it’s the real value independent of the column size allowing to compare different size of columns; for example 100 mL/h used for two columns having a surface doubling will make a factor two for the residence time.
Linear flow rate (cm/h) X surface (cm2) = volumetric flow rate (ml/h)
In our case with the XK50 column (diameter = 5 cm surface = 19.63 cm2
31 cm/h = 608 mL/h; 15 cm/h = 294 mL/h

6. l. 122: it is not clear what is meant by "three-dimensional environment with 30% of alpha-helix". Please re-phrase to make the sentence clear.
R: The sentence was changed.

7. l. 127: "CAPS" needs to be defined.
Done

8. l. 197-202. "KDa" should be corrected to "kDa".
Done; also in figure legends.

9. l. 213: missing blank.
Added

10. l. 229: define "mDAP"
Done

11. l. 264-264: What is meant by "...and the conformation of the segment 402-420 are conserved in all PBPs."? What is meant here with "conformation"? Also, you need to clarify if the "conformation" is conserved in all known PBP structures, or in all class B PBPs, or what is meant here.
R: The sentence was modified

12. l. 284. Here, it does not become clear why the comparison with other PBPs provides evidence for flexible junction between the modules. What is the evidence, and

how has it been obtained? Also, have other computational methods been used to assess the flexibility?

R: Evidence is suggested also by apo and acyl structures of PBP3 from Pseudomonas aeruginosa (Sainsbury, JMB, 405, 173-184). The flexibility of the junction also exists in class A PBPs. We have modified the sentence, added a figure as suggested by reviewer 3 remark 9, and added references.

13. l. 287: what is meant with "processive displacement of the divisome"?

R: It means divisome displacement during processive glycan chain synthesis. The sentence has been simplified

14. l. 298: should be "Marrec-Farley" with capitol "F".
OK (Marrec-Fairley)

15. l. 425. It must be clearly stated in the heading of the legend and in part (a) that the figure shows a model of the PBP3 structure, and not the crystal structure itself (as is written).
R: The figure was modified according to reviewer3's suggestion showing now the crystal structure in cartoon and a light trace of the modelled loops.

16. l. 431. should be "Tyr".
OK

17. Figure 1: should it be "Loop 202-228" (instead of "Loop 220-228") to be consistent with the text?
R: The correction was done in figure 1

Reviewer #3:
1. Analysis of Figure 1 gives the reader the impression that the structure includes the transmembrane region, as well as the full N-terminal domain. Reading of the figure legend, however, indicates that the TM was modeled, and so were all of the regions in cyan. Since this is a very important figure for the paper, and could be eventually used by other scientists for teaching, etc, it should only include the regions that could be traced in a trustworthy fashion in the map. The TM region does not have to be included (it is not helpful for the figure, or even mentioned in the text), and all loops and regions that were modeled should be replaced by dots.

R: The figure has been modified as suggested by the reviewer. The modeled loops are now shown in very light grey and the TM helix has been removed. We have also followed the reviewer's remark 15 suggesting showing beta-strands colored differently from alpha-helices.

2. It is unclear to the reader why authors started their clone at residue 57; a schematic figure could be included, describing the exact construct that was used and the structure that was traced.

R: The construct starting at residue 57 was less prone to degradation that a construct starting at residue 37. See Fraipont C et al. (1994) Engineering and overexpression of periplasmic forms of the penicillin-binding protein 3 of Escherichia coli. Biochem J 298 ( Pt 1): 189-195. The reference has been added in the material and method section. Figure 1 now clearly shows the construct and the difference between what was seen in the map and the modeled loops.

3. P. 10, lines 220-221, it is rather strange to mention that the C-terminus is associated to the N-terminus; do authors mean to say that it interacts closely?
R: The sentence has been made clearer.

4. Although one has the impression that there are 4 individual figures, in fact they are only 2, parts A and B of the same figure having been separated into different files. As a consequence, this manuscript only has 2 figures. Authors could illustrate their manuscript better by adding additional figures; for example, showing the 'long groove'

| | |
|---|---|
| | that is alluded to on p. 10, lines 227-228.<br><br>R: We have added some figures: a model with part of the substrate showing the long groove (remark 5) and a figure showing the superposition of different class B-PBPs (remark 9). We have included the supplementary figures in the manuscript.<br>Figure 1: structure of PBP3<br>Figure 2: Active site<br>Figure 3: Junction<br>Figure 4: Domain 88-165<br>Figure 5 : PBP3 oligomerization<br>Figure 6 : Interaction with peptidoglycan<br><br>5. There is a paper from the Mobashery lab describing the structure of an E. coli PBP (5/6) with a peptide in the active site; since authors mention that their long groove could bind substrate, how does it compare to this paper? Is it possible to model a peptide in their structure?<br><br>R: We have modeled the acyl-enzyme with D-Glu-mDap-D-Ala linked to the active serine and made a figure of it. The model is based on an unpublished acyl-enzyme structure that we have obtained with another PBP (the DD-peptidase from Actinomadura R39) rather than the Mobashery's one, which has a lysine instead of diaminopimelic acid in the peptide<br><br>6. P.10, after lines 223-224, a reference should be cited.<br><br>R: As lines 223-224 are empty, we believe that reviewer's remark relates to lines 233-234, where we have added a reference.<br><br>7. P.12, this part of the text refers to figure 1b, which is rather problematic. Details about a pocket are described, but by looking at the figure one does not have the impression to see a pocket; since one of the beta-strands was shown as sticks (which is not really helpful), it gives the reader the impression that there is a peptide bound to the active site. In order to make this clearer, authors should show the active site with arrows for beta strands (that should be labeled as per other PBPs … the beta-strands neighboring the active site on this figure are beta3 and beta4).<br><br>R: There are now two figures showing the active site. The first (figure 2a) shows the groove (cf remark 5) and the second is the former figure 1b (now 2b) modified as suggested by the reviewer (strand beta3 shown as a strand and labeled). Both are in stereo (cf remark 13)<br><br>8. P.12, lines 269-270: please mention the nomenclature for the beta strands involved, and add references here.<br>R: Nomenclature and references have been added<br><br>9. P.12, lines 283-284: these interesting sentences could be illustrated by a figure highlighting the differences between junctions for different PBPs (and references should also be added)<br><br>R: Details were added to the text and a new figure illustrates these sentences (figure 3).<br>10. 9. P. 14, line 310, please replace 'tridimensional' by 'three-dimensional'<br>Done<br><br>11. If authors only have 2 figures in their manuscript, why did they include three supplementary figures? All of the data can be included in the main text.<br>We have integrated all the figures in the manuscript<br><br>12. It is curious that on p. 16 lines 374-375 authors discuss the fact that a role for domain swapping in the in vivo dimerization process of PBP3 is elusive, and in lines 380-381 go on to discuss that their could be a role for this in vivo.<br><br>R: In lines 380-381, we mention the possible influence of the in vitro dimerization of domain 88-165 on the result of interaction tests. We have slightly modified the |

| | |
|---|---|
| | sentence to avoid confusion<br><br>13. Figure 1, legend: this reviewer recommends that secondary strand elements be labeled, as suggested above. What do authors mean by 'unhide' Tyr514? If their objective is to show it clearly, they could potentially change the angle, or make a stereo figure, or make a LigPlot figure ...<br>R: See remark 7<br><br>14. I'm not quite sure how relevant Fig. 2b is, especially considering that authors clearly mention that these interactions are probably not relevant in the full-length PBP3 structure. They could potentially replace it by supplementary data, or other images of the full-length crystal structure. What does a surface charge diagram look like?<br><br>R: We have kept this illustration, which makes the description of the swapping easier to understand.<br><br>15. These authors published a beautiful review article in FEMS a few years ago where they showed the transpeptidase domain of PBPs with beta-strands colored differently from alpha-helices; they could perhaps adopt that strategy for this paper, and modify Figs. 1a/1b accordingly.<br><br>R: We have modified figure 1 as suggested |
| **Additional Information:** | |
| **Question** | **Response** |
| **Competing Interest**<br><br>For yourself and on behalf of all the authors of this manuscript, please declare below any competing interests as described in the "PLoS Policy on Declaration and Evaluation of Competing Interests."<br><br>You are responsible for recognizing and disclosing on behalf of all authors any competing interest that could be perceived to bias their work, acknowledging all financial support and any other relevant financial or competing interests.<br><br>If no competing interests exist, enter: "The authors have declared that no competing interests exist."<br><br>If you have competing interests to declare, please fill out the text box completing the following statement: "I have read the journal's policy and have the following conflicts"<br><br>* typeset | "The authors have declared that no competing interests exist." |

| | |
|---|---|
| **Financial Disclosure**<br><br>Describe the sources of funding that have supported the work. Please include relevant grant numbers and the URL of any funder's website. Please also include this sentence: "The funders had no role in study design, data collection and analysis, decision to publish, or preparation of the manuscript." If this statement is not correct, you must describe the role of any sponsors or funders and amend the aforementioned sentence as needed.<br><br>* typeset | This work was supported in part by the Belgian Program on Interuniversity Poles of Attraction initiated by the Belgian State, Prime Minister's Office, Science Policy programming (IAP no. P6/19), the Fonds de la Recherche Scientifique, (IISN 4.4505.09, IISN 4.4509.11, FRFC 2.4511.06F), the University of Liège (Fonds spéciaux, Crédit classique, C-06/19 and C-09/75), and a return grant to AD. M. J. is recipient of a FRIA (Fonds de la Recherche pour l'Industrie et l'Agriculture) fellowship (F.R.S.-FNRS, Brussels, Belgium). FK is research associates of the FRS-FNRS, Belgium. The funders had no role in study design, data collection and analysis, decision to publish, or preparation of the manuscript. |
| **Ethics Statement**<br><br>All research involving human participants must have been approved by the authors' institutional review board or equivalent committee(s) and that board must be named by the authors in the manuscript. For research involving human participants, informed consent must have been obtained (or the reason for lack of consent explained, e.g. the data were analyzed anonymously) and all clinical investigation must have been conducted according to the principles expressed in the Declaration of Helsinki. Authors should submit a statement from their ethics committee or institutional review board indicating the approval of the research. We also encourage authors to submit a sample of a patient consent form and may require submission of completed forms on particular occasions.<br><br>All animal work must have been conducted according to relevant national and international guidelines. In accordance with the recommendations of the Weatherall report, "The use of non-human primates in research" we specifically require authors to include details of animal welfare and steps taken to ameliorate suffering in all work involving non-human primates. The relevant guidelines followed and the committee that approved the study should be identified in the ethics statement.<br><br>Please enter your ethics statement below and place the same text at the beginning of the Methods section of your manuscript (with the subheading Ethics Statement). Enter "N/A" if you do not require an ethics statement. | N/A |

Dear Editors:

Please find attached the revised manuscript of a paper titled “Crystal structure of penicillin-binding protein 3 (PBP3) from *Escherichia coli*”.

We have tried to address the concerns of reviewer 1 about the structure. Typographical errors found mainly by reviewer 2 have been corrected and the paper was read by an English native speaker. Finally, as suggested by reviewer 3, we have expanded the description of the structure and modified the figures accordingly. Details can be found in the response to reviewers.

Please modify the Competing Interest by adding the following lines:
Jacques Dumas is employed by Sanofi-Aventis.
This does not alter our adherence to PLOS ONE policies on sharing data and materials.

We look forward to the results of your review.

Sincerely,

Dr Eric Sauvage

Address: Centre d’Ingénierie des Protéines
Université de Liège
B-4000 Sart Tilman, Liège
Belgium
Phone: +3243663620
Fax : +3243663364
Email: eric.sauvage@ulg.ac.be

# Crystal structure of penicillin-binding protein 3 (PBP3) from *Escherichia coli*

Eric Sauvage [1§]*, Adeline Derouaux [1§], Claudine Fraipont [1], Marine Joris [1], Raphaël Herman [1], Mathieu Rocaboy [1], Marie Schloesser [1], Jacques Dumas [2], Frédéric Kerff [1], Martine Nguyen-Distèche [1] and Paulette Charlier [1].

[1] Centre d'Ingénierie des Protéines, Université de Liège, Institut de Physique B5a et Institut de Chimie B6a, Sart Tilman, B-4000 Liège, Belgium,

[2] Sanofi R&D, protein production, 13 quai Jules Guesde, 94403 Vitry sur Seine, France

Running Title: Structure of *Escherichia coli* PBP3

Corresponding author: Eric Sauvage, Centre d'Ingénierie des Protéines, Université de Liège, Institut de Physique B5, B-4000 Liège, Belgium, Tel: +32 4 366 36 20; Fax: +32 4 366 33 64; E-mail: Eric.Sauvage@ulg.ac.be

§ These two authors contributed equally to the work.

**Abstract**

In *Escherichia coli*, penicillin-binding protein 3 (PBP3), also known as FtsI, is a central component of the divisome, catalyzing cross-linking of the cell wall peptidoglycan during cell division. PBP3 is mainly periplasmic, with a 23 residues cytoplasmic tail and a single transmembrane helix. We have solved the crystal structure of a soluble form of PBP3 ($PBP3_{57-577}$) at 2.5 Å revealing the two modules of high molecular weight class B PBPs, a carboxy terminal module exhibiting transpeptidase activity and an amino terminal module of unknown function. To gain additional insight, the PBP3 Val88-Ser165 subdomain ($PBP3_{88-165}$), for which the electron density is poorly defined in the PBP3 crystal, was produced and its structure solved by SAD phasing at 2.1 Å. The structure shows a three dimensional domain swapping with a β-strand of one molecule inserted between two strands of the paired molecule, suggesting a possible role in $PBP3_{57-577}$ dimerization.

## Introduction

The penicillin-binding proteins (PBPs) synthesize and remodel the cell wall peptidoglycan, a major component of the bacterial cell wall that gives the cell its shape and rigidity [1-4]. They are found in all bacteria and represent major targets in anti-biotherapy, especially for the widely used β-lactam antibiotics. Penicillin-binding proteins belong to the family of acyl-serine transferases and are traditionally separated into high-molecular-weight (HMW) PBPs and low-molecular-weight (LMW) PBPs based on molecular weight and sequence homology [4-6]. The former enzymes act as transpeptidases *in vivo* and are involved in peptidoglycan synthesis while the latter are carboxypeptidases and endopeptidases [7] thought to remodel peptidoglycan during the bacterial life cycle but details of their *in vivo* activities are not well established. The HMW-PBPs group can be subdivided into classes A and B, the LMW group into classes A, B and C. Class B HMW-PBPs can be further divided into subclasses and *Escherichia coli* PBP3 is paradigmatic of subclass B3 that groups class B PBPs from Gram negative bacteria involved in cell division. Some PBPs from Gram positive bacteria involved in spore peptidoglycan synthesis also belong to subclass B3, e.g. SpoVD from *Bacillus subtilis*.

During cell division, the peptidoglycan is synthesized by the periplasmic part of a macromolecular complex called the divisome, made up of at least 20 proteins in *Escherichia coli* [8]. Cell division is initiated by the polymerization of tubulin homolog FtsZ into a contractile ring at midcell [9] and the other division proteins are recruited sequentially to the septal ring. FtsZ first associates with FtsA, ZapA and ZipA that stabilize the FtsZ filaments and tether them to the cytoplasmic membrane. The divisome then matures with a long delay between formation of the Z ring and recruitment of the proteins downstream of FtsK[10]. These proteins involved in septal peptidoglycan synthesis are now thought to be recruited as subcomplexes, at least FtsQ/L/B [11] and FtsW/PBP3 [12]. FtsN, which contains a SPOR

peptidoglycan binding domain, is the last essential division protein that localizes at the septum [13]. Finally, various proteins not essential for septal peptidoglycan synthesis associate with the divisome: the Tol/Pal complex involved in the invagination of the outer membrane [14], and the peptidoglycan hydrolase AmiC (and its activator NlpD) that plays an essential role in the separation of daughter cells [15]. Recently, the outer membrane protein LpoB was also shown to associate with the divisome and to regulate peptidoglycan synthesis by interacting with the glycan chain polymerase/transpeptidase PBP1b [16].

In *E. coli*, PBP3 (FtsI) is an essential protein of the divisome, catalyzing peptide cross-bridges between the glycan chains of the peptidoglycan. PBP3 is involved in many interactions within the divisome. It interacts directly with PBP1b which localizes at the division site during septation in a PBP3 dependent fashion [17]. PBP3 works in concert with PBP1b to incorporate the nascent glycan chain into the existing peptidoglycan [4]. The N-terminal 56 residues of PBP3 (containing a cytoplasmic peptide, the transmembrane segment and a short periplasmic peptide) interact with PBP1b in a two-hybrid assay. However other interacting sites should be present in the periplasmic part of PBP1b and PBP3 [17]. PBP3 also interacts directly with FtsW and with FtsN, which itself interacts with PBP1b and stimulates its activity [18]. These proteins are able to form a discrete complex independently of the other cell division proteins [12]. Interaction of PBP3 with FtsA, FtsK, FtsQ [19] or FtsL [20] were also reported but the structural details and the sites of interaction between PBP3 and the proteins of the divisome remain to be elucidated.

The *ftsI* gene encodes a 588 residues protein but proteolytic cleavage removes 11 amino acids at the C-terminal part of the protein[21]. We have solved the crystal structure of the periplasmic domain of PBP3 (residues 57-577) at 2.5 Å. We have also produced, purified, crystallized and solved the structure of the Val88-Ser165 subdomain ($PBP3_{88\text{-}165}$), a potential

protein-protein interaction domain, which was poorly defined in the electron density map of $PBP3_{57-577}$.

## Material and Methods

**Bacterial strains, oligonucleotides and media:** Bacterial strains were *E. coli* Top 10F' for cloning (Invitrogen, USA) and *E. coli* C41(DE3) for expression [22]. Oligonucleotides were from Eurogentec. The rich media used were 2XYT (bacto-tryptone 16 g, yeast extract 10 g, NaCl 5 g, water 1 l, pH 7.0.) or Luria-Bertani (LB) medium supplemented with ampicillin (100 µg $ml^{-1}$), chloramphenicol (20 or 30 µg $ml^{-1}$), kanamycin (50 µg $ml^{-1)}$ and IPTG (0.5 mM) when appropriate.

**$PBP3_{57-577}$: Production, purification, crystallization, data collection and structure refinement.**

Plasmids used were pDML232 for the PBP3 and pDML237 for SecB[23]. Fermentation of *E. coli* strain W3110M was performed in RFB MIL11/03 at 37°C to overexpress the PBP3(57-577), allowing to obtain soluble protein expression at 210 mg/l of culture.

50 g of wet bacterial pellet corresponding to 1 litre of culture were suspended into 150 ml of 100 mM Tris (pH 8), 0.1 mM PMSF buffer, under magnetic stirring in an ice batch for 30 minutes. Mechanical lysis of bacteria was performed with a Rannie at 650 bars and cooling. Cell lysate was centrifuged on a JOUAN SR 20.22 at 42 000 g for 1 hour at 4°C. We then centrifuged the supernatant on a Beckman XL90 at 100 000 g for 30 minutes at 4°C, in order to clarify the solution.

The clarified supernatant was loaded on a S-Sepharose Fast Flow column (XK50/30) equilibrated with buffer A (100 mM Tris (pH 8), 10% glycerol, 10% ethylene glycol) at 608

ml/h. Elution was performed with a linear gradient from 100% of buffer A to 40% of buffer B (buffer A + 1 M Nacl). PBP3 was eluted at about 20% of buffer B. Eluate was diluted 1/3 in buffer A and loaded on an S-Sepharose Hiload (XK16/10) column equilibrated in buffer A at 588 ml/h. Elution was performed with buffer C (100 mM Tris (pH 8), 10% glycerol, 10% ethylene glycol, 0.5 M NaCl). The eluate collected in one column volume was then purified on a Superdex 200 (XK50/60) column at 294 ml/h to obtain a highly purified and homogenous protein. 120 mg of purified protein were obtained at 1.6 mg/ml (UV measurement). N-terminal sequence was checked and confirmed. Circular dichroism analyses showed that the protein has a stable three-dimensional structure with 30% of alpha-helix. The FRET (resonance energy transfer) measurements showed a rotational coefficient of 38 ns which demonstrated the monodisperse status of the population with an apparent molecular weight of 53 KDa.

Crystals of $PBP3_{57\text{-}577}$ were grown at 20°C by hanging drop vapor diffusion. Crystals were obtained by mixing 5 µl of a 18 mg/ml protein solution (also containing 0.5 M NaCl and 20 mM Tris, pH 8), 4 µl of well solution (2.5 M ammonium sulfate and 0.1 M N-cyclohexyl-3-aminopropanesulfonic acid (CAPS), pH 10), and 1 µl of 0.1 M NaCl solution. Crystals appeared after several months and the apparent very narrow range of crystallization conditions resulted in only some very small badly diffracting crystals and one crystal diffracting at 2.5 Å. Diffraction data were measured on Beamline ID29 at the European Synchrotron Radiation Facility (ESRF, Grenoble, France) and processed using Mosflm [24] and SCALA from the CCP4 program suite. [25] The structure of PBP3 was solved by molecular replacement with the program PHASER [26] using the structure of PBP2 from *Neisseria gonorrhoeae* (PDB id: 3equ) as the initial search model. Refinement was carried out using REFMAC5, [27] TLS, [28] and Coot. [29]. The final refinement statistics are given in Table 1.

**PBP3$_{88-165}$: Production, purification, crystallization, data collection and structure refinement.**

The *ftsI* fragment encoding PBP3$_{88-165}$ was amplified by PCR using plasmid pMVRI [17] as template and oligonucleotides 5'-GGACCCGGGGTAAAAGCGATTTGGGCTGACCC-3' and 5'-GCCGGATCCTTAAGAC TCTTCACGCAGATGAATCCC-3' as primers (*XmaI* and *BamHI* are underlined). The PCR fragment was cloned into the pJet1.2/blunt cloning vector (Fermentas), sequenced, digested with *XmaI* and *BamHI* and inserted into the same sites of plasmid pET-52b(+). The resulting plasmid pDML2042 codes for the PBP3$_{88-165}$ with an N-terminal strep-tag. The strep-tag- PBP3$_{88-165}$ was isolated from *E. coli* C41(DE3) harbouring pDML2042 grown at 37° C in 2XYT medium in the presence of 0.5 mM IPTG for 3h. The harvested cells were suspended in 40 ml of 100 mM Tris-HCl pH 8.0, 150 mM NaCl, 1mM EDTA containing a protease inhibitor cocktail (Roche) (buffer C), broken 5 times into a high-pressure homogenizer (Emulsiflex-C3 Avestin Inc.) and centrifuged at 25000g for 40 min. The supernatant was filtered (0.45µ) and applied to a 5 ml *Strep*-Tactin IBA column. After 5 washes with buffer C, the strep-tag-PBP3$_{88-165}$ was eluted in 100 mM Tris-HCl pH8.0, 150 mM NaCl, 1mM EDTA, 2.5mM desthiobiotin. The fractions of interest (5ml) were dialyzed against 2 L of buffer C with a 3,500 Dalton cut off membrane and analyzed by SDS-18% PAGE. About 6 mg of PBP3$_{88-165}$ per liter of culture were produced and purified to 90% purity. The strep-tag was removed from PBP3$_{88-165}$ before crystallization.

Crystals of PBP3$_{88-165}$ were grown at 20°C by hanging drop vapor diffusion. Crystals were obtained by mixing 4 µl of a 7.5 mg/ml protein solution containing 0.15 M NaCl and 0.1 M Tris, pH 8 1mM EDTA, and 1 µl of well solution (2 M ammonium sulfate and 0.1 M citrate, pH 3.5). The structure of PBP3$_{88-165}$ was solved by single anomalous diffraction using a selenomethionine substituted SePBP3$_{88-165}$ crystal. Selenomethionine substituted SePBP3$_{88-165}$

was expressed by using minimal medium supplemented with selenomethionine and purified and crystallized as $PBP3_{88-165}$. Diffraction data for the $SePBP3_{88-165}$ crystals were measured on Beamline PROXIMA 1 at SOLEIL (Paris, France). Data were processed using XDS [30] and initial structure determination of $SePBP3_{88-165}$ was determined with the help of SHELXC/D/E [31], Parrott [32] and Buccaneer [33].

Refinement was carried out on native $PBP3_{88-165}$ using REFMAC5, [27] TLS, [28] and Coot. [29]. Diffraction data for the native $PBP3_{88-165}$ were measured on Beamline BM30A at the European Synchrotron Radiation Facility (ESRF, Grenoble, France) and processed using Mosflm [24] and SCALA from the CCP4 program suite. [25] Data and final refinement statistics are given in Table 1.

**Western blotting:** Western blotting was carried out as described [12]. PBP3, PBP1b and FtsN were revealed with respective polyclonal antibodies and FtsW was probed with monoclonal anti-HA-Peroxydase (HighAffinity (3F10) Roche).

.

**Light Scattering (DLS and SLS).**

Dynamic and static light scattering data were recorded on a DynaPro NanoStar instrument (Wyatt Technology Corporation) operated in batch mode at 20°C and fitted with a laser beam emitting at 658 nm with power auto-attenuation. Scattering angles were 90° for both DLS (avalanche photodiode) and SLS (silicon PIN photodetector). Measurements were performed under buffer conditions and concentration used for crystallogenesis. Samples were filtered on Whatman Anotop 10 inorganic membrane (0.02 µm cut off) and loaded into a 10 µl quartz microcuvette. Data were averaged from 20 acquisitions of the scattered light intensity during 5 s, with a sum of squares error value below 100. Scattering data were analyzed using DYNAMICS v. 7.1.1.3 software (Wyatt Technology Corp.) that includes the DYNALS

module for distribution analysis in photon correlation spectroscopy. A globular protein model was used for mass estimation in DLS and a dn/dc value of 0.185 ml/g for mass calculations in SLS. Theoretical protein hydrodynamic radii were calculated from pdb files with program HYDROPRO [34].

**Protein binding to peptidoglycan.** Protein binding to peptidoglycan was performed as described in Typas *et al.* [16]. Briefly, 10 µg of protein were incubated with a peptidoglycan suspension of *E. coli* MC1061. The peptidoglycan was pelleted, washed and resuspended in 2% SDS. The unbound fraction, the wash fraction and the resuspended pellet were analysed by SDS-18% PAGE. A control sample was realized without peptidoglycan.

**Gel filtration.** Gel filtration experiments were performed on a Superdex 200 10/300 GL and on a Superdex 75 10/300 GL for $PBP3_{57-577}$ and $PBP3_{88-165}$ respectively. The proteins were used at the same concentration and in the same buffer as in the crystallogenesis assay and in DLS. 200 µl of protein were injected. Standard proteins (lysozyme 14.3 kDa, trypsin inhibitor 20.1 kDa, carbonic anhydrase 31 kDa, bovine serum albumin 66.5 kDa) were used for calibration.

**Accession numbers.** The atomic coordinates for the crystal structure of $PBP3_{57-577}$ and $PBP3_{88-165}$ are available at the Protein Data Bank with the accession numbers PDB ID: **4BJP** and **4BJQ**.

## Results and discussion

### Structure determination

The crystal structure of a soluble form of PBP3, including residues 57 to 577, was solved at 2.5 Å resolution. The structure of PBP3 was solved by molecular replacement using the

structure of PBP2 from *N. gonorrhoeae* (PDB id: 3equ) [35]. PBP3 crystallizes in space group $P6_122$ with one molecule in the asymmetric unit. The structure was built from residues 71 to 567 but absence of detectable electronic density did not allow structure determination for residues 93-112, 119-141, 152-162, 202-228 and 537-543. PBP3 structural information was supplemented by independently solving the Val88-Ser165 subdomain structure (see below). Final $R_{cryst}$ and $R_{free}$ values for the PBP3 structure determination are 19.9 % and 24.5 % respectively.

The overall fold of periplasmic PBP3 is bimodular (Fig. 1). The C-terminal module is responsible for the transpeptidase activity but no clear function has been assigned yet to the N-terminal module of the construct.

**Transpeptidase module and active site**

The C-terminal module shares its overall fold with the transpeptidase domain found in all PBPs [5,36]. Structure-based alignments of the PBP3 transpeptidase domain show little structural deviations from the corresponding domains of class B3 PBPs with r.m.s.deviations of 1.3 Å (Acitenobacter baumanii PBP3 [37]), 1.3 Å (*Pseudomonas aeruginosa* PBP3 [38] and 1.4 Å (*N.gonorrhoeae* PBP2 [35] and larger deviations for class B PBPs from other subgroups (1.7 Å, 2.1 Å, 2.1 Å, and 2.1 Å for *Mycobacterium tuberculosis* PBPA [39], *Streptococcus pneumoniae* PBP2x [40], *S. pneumoniae* PBP2b [41] and *Staphylococcus aureus* PBP2a [42], respectively). The active site responsible for the transpeptidase activity of PBP3 is located in a long groove that can accommodate the carboxy-terminal residues of the PBP3 natural substrate, the peptidoglycan stem pentapeptide L-Ala-γ-D-Glu-meso-diaminopimelic acid (mDAP)-D-Ala-D-Ala (Fig 2a).

The transpeptidase activity of PBP3 relies on eight residues, Ser307, Lys310, Ser359, Asn361, Lys494, Thr495, Gly496 and Thr497, found with few exceptions in all penicillin-binding enzymes (Fig. 2b). These residues form three conserved sequence motifs (Ser-Xaa-

Xaa-Lys, Ser-Xaa-Asn and Lys-Thr-Gly-Thr) and are also responsible for the binding of β-lactam antibiotics to the active site of PBPs [5].

The mechanism leading to linkage between the stem peptides of two glycan chains involves an acyl-enzyme formed between the active serine and the penultimate D-Ala of one stem peptide, releasing the ultimate D-Ala. In this mechanism, the nucleophylicity of the active serine Ser307 would be enhanced by Lys310, and Ser359 would be important for back-donation of the proton to the active serine during the acylation step. Deacylation involves the attack of the acyl bond by the free amine group of a second stem peptide diaminopimelic acid. Lys494 could play an important role in deacylation in concert with Ser359, as suggested for other PBPs [43-45].

Asn361 should be important for proper positioning of the interpeptidic amide group linking the penultimate D-Ala to the diaminopimelic acid residue. Substitution of Asn361 by a serine causes a dramatic change in pole shape [46]. The pointed polar caps observed in the *E. coli* mutant harboring this mutation appeared to be associated with the activity of PBP3. Asn361 differentiates PBP3 from its elongation homologue PBP2. The presence of an aspartic acid at this position in *E. coli* PBP2 and more generally in all PBPs of class B2( which contains Gram negative class B PBPs associated to elongation) is a noticeable exception to the conservation of this residue in peptidoglycan synthesizing PBPs. The nature of the amino-acid should be of importance for the fine structural conformation of peptidoglycan.

Finally, both threonine residues of the Lys-Thr-Gly-Thr motif should serve as an anchor to the C-terminal carboxylate group of the pentapeptide. They are found hydrogen bonded to the penultimate D-Ala carboxylate in structures of DD-peptidases in complex with peptide fragments [45,47].

In all ligand-free PBP-structures a water molecule is observed in the oxyanion hole. In PBP3, the oxyanion hole, defined by the amine groups of residues 307 and 497, is unexpectedly

occupied by the hydroxyl group of Tyr514 that is at 2.7 Å from Ser307N and 3.25 Å from Thr497N (Fig. 2b). Sequence alignment shows that Tyr514 is unique to PBP3 among class B PBPs. The side chain of Tyr514 is free to easily rotate and liberate the oxyanion hole and should not play a particular role in transpeptidation.

The rear side of the PBP3 active site is made of residues Phe417-Gly-Tyr-Gly (Fig. 2b). The motif Tyr/Phe/Ile-Gly-Tyr/Gln-Gly and the tertiary structure of the segment 402-420 are conserved in each class of PBPs. Gly418 closes a hydrophobic pocket that can accommodate the methyl group of the penultimate D-alanine of the stem pentapeptide, conferring to PBPs a high specificity for a D-alanine as the fourth residue of the pentapeptide.

Electron density around residues 499-510, a loop that connects strands β3 and β4 close to the active site, is weak but sufficient to allow its determination. Disorder of this loop is a general property of class B PBPs whereas in other classes of PBPs, a small hairpin connects the two strands [38,43,47-50]. It could be stabilized by interactions with another protein of the divisome, e.g. for an adequate position and orientation of the active site of PBP3 along with the transpeptidase active site of PBP1b. The loop could also have a role for accompanying the displacement of the glycan chain on the surface of PBP3. In a similar manner, a disordered loop in the glycosyltransferase domain of *S. aureus* PBP2, a class A PBP homologous to PBP1b, was proposed to allow the nascent glycan chain to move processively from the donor site to the acceptor site [51].

**N-terminal module**

The N-terminal module provides three loops (180-190; 202-228; 280-294) and one subdomain (88-165) for potentially interacting with other proteins of the divisome. The residues between these loops and subdomain form a series of motifs well conserved in the primary sequence of class B PBPs [4], forming the junction between the C- and N-terminal modules and tethering

290 the loops from the latter to the C-terminal module. Comparison with the structures of other
291 class B PBPs shows that the relative position between the two modules can vary, suggesting
292 that the junction between both modules is flexible. Difference between apo and acyl-enzyme
293 structures of *P. aeruginosa* PBP3 led to the same conclusion [38]. Figure 3 shows the
294 structures of *S. aureus* PBP2a [42] and *S. pneumoniae* PBP2b [41], with their C-terminal
295 domain superposed onto that of PBP3, highlighting the fact that the domains equivalent to
296 $PBP3_{88\text{-}165}$ (domain 169-237 for SauPBP2a and domain 104-197 for SpnPBP2b) lie in
297 different position. Class A PBPs also show a high degree of flexibility between their
298 glycosyltansferase module and the ensemble made of the linker and the transpeptidase module
299 [51]. Such flexibility could be necessary for the enzyme to reach its target or be required for
300 displacement of the divisome along the septum.
301 The 180-190 loop forms a small β-hairpin exposing Val184 and Asp185 to the solvent. The
302 length of this loop is characteristic of class B PBPs pertaining to the divisome (PBP3) and is
303 much longer in class B PBPs acting during elongation (PBP2). The 280-294 loop, from the C-
304 terminal module, is close to the 180-190 loop and is also longer in the PBPs of the elongation
305 complex than in the PBPs of the divisome. These two loops could thus represent a specific
306 PBP3 zone of interaction with partners of the divisome, preventing PBP3 to associate with
307 proteins of the elongation complex or, conversely, preventing PBP2 to associate with proteins
308 of the divisome.
309 Electron density is absent for segment 202-228, which again suggests that interactions with a
310 partner protein may stabilize its tertiary structure in the divisome. Marrec-Fairley *et al.* [52]
311 have characterized mutants of the E206-V217 segment consistent with such a role in protein
312 interaction. R210 seems particularly important, together with residues G57, S61 and L62, for
313 the recruitment of FtsN [53].
314

**PBP3$_{88\text{-}165}$ subdomain**

Electron density was very poor for residues between Val88 and Ser185, with only some secondary structures showing up in the electron density maps. Apparent disorder of domain 88-165 is also observed in *N. gonorrhoeae* PBP2 [35] and to a lesser extent in *Pseudomonas aeruginosa* PBP3 [38], *Acinetobacter Baumanii* PBP3 [37], *Enterococcus faecium* PBP5 [54] and *S. pneumoniae* PBP2x [40], all of which are class B PBPs. Interaction of this domain with another protein of the divisome may stabilize its tertiary structure. In order to determine its three-dimensional structure, the PBP3$_{88\text{-}165}$ domain was produced and its structure solved.

The domain crystallizes in P1 with eight molecules in the asymmetric unit. Because of the high number of copies in the asymmetric unit, molecular replacement using the closely related domain Val79-Phe151 of *P. aeruginosa* PBP3 failed to provide a solution, whatever the Molecular Replacement program used. The structure of the PBP3$_{88\text{-}165}$ domain was eventually determined by single anomalous diffraction using a selenomethionine substituted PBP3$_{88\text{-}165}$ crystal and refined over data collected on a crystal of the native PBP3$_{88\text{-}165}$ protein. The electron density is well defined except for residues 132-135 in chain F and for the C-terminal residue in chains E, G and H. Final Rwork and Rfree values for the PBP3$_{88\text{-}165}$ domain are 20.9 % and 26.3 % respectively. The eight molecules in the asymmetric unit are organized in four pairs with, in each pair, 18 N-terminal residues swapping into the paired molecule (Fig. 4a). The swapped residues represent a two-turn helix and a β-strand that inserts between two β-strands of the other molecule to form a three stranded β-sheet. Interactions between the two molecules are numerous and include many hydrogen bonds, salt bridges (e.g. for associated chains A and C: Asp94A-Arg135C, Glu97A-His160C), hydrophobic clusters (Ile91A is surrounded by seven leucines or isoleucines from chain C), and an aromatic ring stacking (Trp92A is sandwiched between Phe136C and His160C) (Fig. 4b). Together, residues 88-105 from one molecule and residues 106-165 from the paired molecule form a small globular

domain whose tertiary structure, three anti-parallel β-strands flanked by three helices, is homologous to the equivalent domain of *P. aeruginosa* PBP3.

Mutations in the *E. hirae* $PBP5_{190-261}$ domain, homologous to $PBP3_{88-165}$, support the hypothesis that this domain is a good candidate to play a role in protein-protein interactions [55]. Of note is the insertion of 60 residues assembling in four helices in the corresponding domain of PBPs of subclass B5 [41,56].

**PBP3 dimers.**

PBP3 dimerization was shown *in viv*o by two-hybrid assay [19,20] and FRET [12], and the structure of $PBP3_{88-157}$ suggests that PBP3 dimerization could be reinforced by 3D domain swapping involving residues 88-105. The weak electronic density around domain 88-165 in the crystal of $PBP3_{57-577}$ allows the approximate positioning of $PBP3_{88-165}$ structure in the crystal of $PBP3_{57-577}$. $PBP3_{88-165}$ then faces a symmetric domain with the crystallographic axis of symmetry at the hinge point where domain swapping occurs in $PBP3_{88-165}$, raising the possibility that swapping also occurs in the crystal of $PBP3_{57-577}$. Domain swapping in $PBP3_{57-577}$ would yet involve a twisting of $PBP3_{88-165}$ domain, i.e. symmetrical $PBP3_{88-165}$ domains would not be oriented in the $PBP3_{57-577}$ crystal in the same manner as in the $PBP3_{88-165}$ one.

The oligomerization state of $PBP3_{88-165}$ and $PBP3_{57-577}$ was investigated by Light Scattering and gel filtration. DLS and SLS experiments carried out on a solution of $PBP3_{88-165}$ suggested a dimer in solution. The monodisperse distribution observed in DLS provided a hydrodynamic radius of 18 Å corresponding to the radius of the $PBP3_{88-165}$ dimeric form calculated from the coordinate file whereas the average molecular mass given by SLS was 27 kDa, which is an overestimated mass of $PBP3_{88-165}$ dimer due to the strong influence of small quantities of remaining aggregates on mass calculation. Gel filtration assays carried out with $PBP3_{88-165}$

provided 2 peaks representing each 50% of the total protein content (Fig. 5a). The second peak represents $PBP3_{88-165}$ dimers and the first peak accounts for higher order multimers. From these results, we conclude that, at the concentration used for crystallization, monomers of $PBP3_{88-165}$ are absent and dimers are predominant in the solution.

DLS analysis of $PBP3_{57-577}$ exhibited unimodal particle-size distributions with an intensity-average hydrodynamic diameter of 48 Å. Hydrodynamic radii calculated from pdb files gives 27 Å and 54 Å for a monomer or a dimer of $PBP3_{57-577}$ respectively, suggesting that a dimer is predominant in solution. This was confirmed by SLS analysis, which provided a molecular mass of 108 kDa, corresponding to a $PBP3_{57-577}$ dimer. In gel filtration assays, $PBP3_{57-577}$ was mainly eluted as a monomer with 5% of dimers (Fig. 5b), which might be explained by the constant displacement of the equilibrium toward the monomer when it is separated by the size from the dimer. At the concentration used for crystallization, dimers of $PBP3_{57-577}$ can predominate in the solution but monomers are also present and it remains unclear if $PBP3_{57-577}$ dimerization results directly from 3D domain swapping.

3D domain swapping is frequently observed as an artefact resulting from crystallization, without bearing relevance to biological function. Because domain swapping in the $PBP3_{57-577}$ crystal would involve a large twisting of the (88-165) domain and, also, because domain swapping should stabilize the domain and hence provide a clear electronic density in that region, the domain swapping observed in the case of $PBP3_{88-165}$ is probably absent in the $PBP3_{57-577}$ crystal. Moreover, in the full PBP3, domain swapping would extend from residue 105 to the amino terminus and swapping of such a large domain has never been reported. A role for domain swapping in the *in vivo* dimerization of PBP3 seems therefore elusive.

**$PBP3_{88-165}$ interactions**

PBP1b, FtsN or FtsW are known to interact with PBP3 but a direct interaction between these proteins and the $PBP3_{88-165}$ domain could not be detected using affinity chromatography (data not shown). Nevertheless, $PBP3_{88-165}$ *in vitro* dimerization by domain swapping could impair the interaction, if any, of the $PBP3_{88-165}$ domain with one of these proteins and an *in vivo* interaction of the domain with PBP1b, FtsN or FtsW cannot be discarded.

The subcomplex FtsQ/FtsL/FtsB could also be involved in the interaction with $PBP3_{88-165}$. The N-terminal module of PBP3 appears to interact with FtsL in a two-hybrid system [20]. Lytic transglycosylases represent other potential candidates for an interaction with $PBP3_{88-165}$. In *E. coli*, the soluble lytic transglycosylase Slt70 was shown to interact with PBP3 [57], whereas in *N. meningiditis* the membrane bound lytic transglycosylase MltA was shown to interact with PBP2Ng [58], the orthologue of *E. coli* PBP3.

We tested the possibility that the $PBP3_{88-165}$ domain could interact with the peptidoglycan. The binding of $PBP3_{57-577}$ and $PBP3_{88-165}$ to peptidoglycan sacculi was tested by a pull-down assay (Fig. 6). We showed that a part of $PBP3_{57-577,}$ but not $PBP3_{88-165}$, was pelleted with the sacculi indicating that it has an affinity for the peptidoglycan. On the whole, results indicate that this region of PBP3 is not essential for its interaction with the murein sacculus although $PBP3_{88-165}$ dimerization could also perturb a possible interaction with the peptidoglycan.

## Conclusion

PBP3 interacts with many proteins and occupies a central role in the periplasmic component of the divisome. The structural information brought by the resolution of the PBP3 structure adds to the available structures of *E. coli* PBP1b, FtsQ, and FtsN carboxy terminal domain.

The modular organisation and the non-folded nature of the small loops or subdomains composing the PBP3 N-terminal module suggest that the latter could be involved in protein-protein interactions with partners of the divisome.

414 The structure of the $PBP3_{88-165}$ domain, disordered in PBP3, shows a dimerization of the
415 domain by three dimensional domain swapping that is possible but unlikely in the full length
416 PBP3. Domain swapping in $PBP3_{88-165}$ domain is unlikely to play a role in the *in vivo* PBP3
417 dimerization and a role in protein-protein interaction remains the most attractive hypothesis
418 for this small domain.
419

**Acknowledgments**

We thank Andy Thompson for his help on Beamlines Proxima1 (SOLEIL) and ID29 (ESRF), Jean – Luc Ferrer for his help on BM30a (ESRF), Maxime Lampilas and Joszef Aszodi for their participation in the PBP3 production and Georges Feller for his expertise with SLS/DLS.

**Figure legends**

**Figure 1 Structure of *E. coli* PBP3.** Cartoon representation of the crystal structure of $PBP3_{57-577}$. A ribbon trace of modelled loops undefined in the crystal structure is shown in grey. The active site is indicated by a red sphere. Loops discussed in the text are indicated.

**Figure 2 PBP3 active site**. (a) Stereo view of a modelled tripeptide D-Glu-mDap-D-Ala in the active site of PBP3. The tripeptide (yellow) is modelled as an acyl-enzyme and is bonded to the active serine shown in green. (b) Stereo view of a cartoon representation of the transpeptidase active site of PBP3. The oxyanion hole is defined by the nitrogen atoms of residues 307 and 497. Loop 400-420 is shown in cyan. Nitrogen atoms are shown in blue and oxygen atoms in red.

**Figure 3 Junction between C- and N-terminal modules**. Comparison between the relative orientation of N and C-terminal modules of PBP3 (blue), *S. aureus* PBP2a (magenta) and *S. pneumoniae* PBP2b (green). The C-terminal domain of SaPBP2a and SpnPBP2b are superimposed onto the C-terminal domain of PBP3. SaPBP2a (169-237) and SpnPBP2b (104-197) are equivalent to domain 88-165 of PBP3.

**Figure 4 Domain swapping in $PBP3_{88-165}$.** (a) $PBP3_{88-165}$ crystal unit cell (space group P1). The 8 chains are organized by pairs with 18 swapped residues. (b) Interactions between swapped residues from chains D (yellow) and H (green), including the hydrophobic cluster around Ile91 (Leu139, Ile151, Leu161), salt bridges (Asp94-Arg135, Glu97-His160 and an aromatic ring sandwich (His160-Trp92-Phe136). Some labels are omitted for clarity. Nitrogen atoms are shown in blue and oxygen atoms in red.

**Figure 5 PBP3 oligomerization.** (a) Chromatogram of $PBP3_{88-165}$ gel filtration on a Superdex 75 10/300 GL. The first peak elutes at 12.16 ml and the second at 13.52 ml. Carbonic anhydrase (31 kDa) elutes at 11.05 ml and lysozyme (14kDa) at 15.25 ml (data not shown). The buffer was 0.15 M NaCl and 0.1 M Tris, pH 8 1mM EDTA. (b) Chromatogram of $PBP3_{57-577}$ gel filtration on a Superdex 200 10/300 GL. The first small peak elutes at 13.3 ml, the second at 14.77 ml. Bovine serum albumin used as a standard elutes at 14.12 ml (molecular mass 67 kDa, data not shown). The masses calculated on the basis of the mass standards are 108.5 kDa for the first peak ($PBP3_{57-577}$ dimer) and 58.5 kDa for the second peak ($PBP3_{57-577}$ monomer). The buffer was 20mM Tris HCl pH 8, 0.5 M NaCl.

**Figure 6**. **Interaction with peptidoglycan**. Pulldown of $PBP3_{57-577}$ (up) and $PBP3_{88-165}$ (down) with and without peptidoglycan sacculi (+ PG and – PG respectively). S, supernatant, W, washing step, P, pellet.

## References


1. Vollmer W, Blanot D, de Pedro MA (2008) Peptidoglycan structure and architecture. FEMS Microbiol Rev 32: 149-167.
2. Young KD (2003) Bacterial shape. Mol Microbiol 49: 571-580.
3. Spratt BG, Pardee AB (1975) Penicillin-binding proteins and cell shape in E. coli. Nature 254: 516-517.
4. Sauvage E, Kerff F, Terrak M, Ayala JA, Charlier P (2008) The penicillin-binding proteins: structure and role in peptidoglycan biosynthesis. FEMS Microbiol Rev 32: 234-258.
5. Ghuysen JM (1991) Serine beta-lactamases and penicillin-binding proteins. Annu Rev Microbiol 45: 37-67.
6. Macheboeuf P, Contreras-Martel C, Job V, Dideberg O, Dessen A (2006) Penicillin binding proteins: key players in bacterial cell cycle and drug resistance processes. FEMS Microbiol Rev 30: 673-691.
7. Goffin C, Ghuysen JM (1998) Multimodular penicillin-binding proteins: an enigmatic family of orthologs and paralogs. Microbiol Mol Biol Rev 62: 1079-1093.
8. Errington J, Daniel RA, Scheffers DJ (2003) Cytokinesis in bacteria. Microbiol Mol Biol Rev 67: 52-65, table of contents.
9. Margolin W (2005) FtsZ and the division of prokaryotic cells and organelles. Nat Rev Mol Cell Biol 6: 862-871.
10. Aarsman ME, Piette A, Fraipont C, Vinkenvleugel TM, Nguyen-Disteche M, et al. (2005) Maturation of the *Escherichia col*i divisome occurs in two steps. Mol Microbiol 55: 1631-1645.

11. Buddelmeijer N, Beckwith J (2004) A complex of the *Escherichia coli* cell division proteins FtsL, FtsB and FtsQ forms independently of its localization to the septal region. Mol Microbiol 52: 1315-1327.
12. Fraipont C, Alexeeva S, Wolf B, van der Ploeg R, Schloesser M, et al. (2011) The integral membrane FtsW protein and peptidoglycan synthase PBP3 form a subcomplex in Escherichia coli. Microbiology 157: 251-259.
13. Dai K, Xu Y, Lutkenhaus J (1993) Cloning and characterization of ftsN, an essential cell division gene in Escherichia coli isolated as a multicopy suppressor of ftsA12(Ts). J Bacteriol 175: 3790-3797.
14. Gerding MA, Ogata Y, Pecora ND, Niki H, de Boer PA (2007) The trans-envelope Tol-Pal complex is part of the cell division machinery and required for proper outer-membrane invagination during cell constriction in E. coli. Mol Microbiol 63: 1008-1025.
15. Bernhardt TG, de Boer PA (2003) The Escherichia coli amidase AmiC is a periplasmic septal ring component exported via the twin-arginine transport pathway. Mol Microbiol 48: 1171-1182.
16. Typas A, Banzhaf M, van den Berg van Saparoea B, Verheul J, Biboy J, et al. (2010) Regulation of peptidoglycan synthesis by outer-membrane proteins. Cell 143: 1097-1109.
17. Bertsche U, Kast T, Wolf B, Fraipont C, Aarsman ME, et al. (2006) Interaction between two murein (peptidoglycan) synthases, PBP3 and PBP1B, in *Escherichia coli*. Mol Microbiol 61: 675-690.
18. Muller P, Ewers C, Bertsche U, Anstett M, Kallis T, et al. (2007) The essential cell division protein FtsN interacts with the murein (peptidoglycan) synthase PBP1B in Escherichia coli. J Biol Chem 282: 36394-36402.
19. Di Lallo G, Fagioli M, Barionovi D, Ghelardini P, Paolozzi L (2003) Use of a two-hybrid assay to study the assembly of a complex multicomponent protein machinery: bacterial septosome differentiation. Microbiology 149: 3353-3359.
20. Karimova G, Dautin N, Ladant D (2005) Interaction network among *Escherichia coli* membrane proteins involved in cell division as revealed by bacterial two-hybrid analysis. J Bacteriol 187: 2233-2243.
21. Nagasawa H, Sakagami Y, Suzuki A, Suzuki H, Hara H, et al. (1989) Determination of the cleavage site involved in C-terminal processing of penicillin-binding protein 3 of Escherichia coli. J Bacteriol 171: 5890-5893.
22. Miroux B, Walker JE (1996) Over-production of proteins in Escherichia coli: mutant hosts that allow synthesis of some membrane proteins and globular proteins at high levels. J Mol Biol 260: 289-298.
23. Fraipont C, Adam M, Nguyen-Disteche M, Keck W, Van Beeumen J, et al. (1994) Engineering and overexpression of periplasmic forms of the penicillin-binding protein 3 of Escherichia coli. Biochem J 298 ( Pt 1): 189-195.
24. Leslie AGW (1991) Molecular data processing. Crystallographic Computing 5: 50-61.
25. CCP4 (1994) The CCP4 suite: programs for protein crystallography. Acta Crystallogr D Biol Crystallogr 50: 760-763.
26. McCoy AJ, Grosse-Kunstleve RW, Adams PD, Winn MD, Storoni LC, et al. (2007) Phaser crystallographic software. J Appl Crystallogr 40: 658-674.
27. Murshudov GN, Vagin AA, Dodson EJ (1997) Refinement of macromolecular structures by the maximum-likelihood method. Acta Crystallogr D Biol Crystallogr 53: 240-255.
28. Painter J, Merritt EA (2006) Optimal description of a protein structure in terms of multiple groups undergoing TLS motion. Acta Crystallogr D Biol Crystallogr 62: 439-450.

29. Emsley P, Cowtan K (2004) Coot: model-building tools for molecular graphics. Acta Crystallogr D Biol Crystallogr 60: 2126-2132.
30. Kabsch W (2010) Integration, scaling, space-group assignment and post-refinement. Acta Crystallogr D Biol Crystallogr 66: 133-144.
31. Sheldrick GM (2010) Experimental phasing with SHELXC/D/E: combining chain tracing with density modification. Acta Crystallogr D Biol Crystallogr 66: 479-485.
32. Zhang KY, Cowtan K, Main P (1997) Combining constraints for electron-density modification. Methods Enzymol 277: 53-64.
33. Cowtan K (2006) The Buccaneer software for automated model building. 1. Tracing protein chains. Acta Crystallogr D Biol Crystallogr 62: 1002-1011.
34. Garcia De La Torre J, Huertas ML, Carrasco B (2000) Calculation of hydrodynamic properties of globular proteins from their atomic-level structure. Biophys J 78: 719-730.
35. Powell AJ, Tomberg J, Deacon AM, Nicholas RA, Davies C (2009) Crystal structures of penicillin-binding protein 2 from penicillin-susceptible and -resistant strains of Neisseria gonorrhoeae reveal an unexpectedly subtle mechanism for antibiotic resistance. J Biol Chem 284: 1202-1212.
36. Massova I, Mobashery S (1998) Kinship and diversification of bacterial penicillin-binding proteins and beta-lactamases. Antimicrob Agents Chemother 42: 1-17.
37. Han S, Caspers N, Zaniewski RP, Lacey BM, Tomaras AP, et al. (2011) Distinctive attributes of beta-lactam target proteins in Acinetobacter baumannii relevant to development of new antibiotics. J Am Chem Soc 133: 20536-20545.
38. Sainsbury S, Bird L, Rao V, Shepherd SM, Stuart DI, et al. (2011) Crystal structures of penicillin-binding protein 3 from Pseudomonas aeruginosa: comparison of native and antibiotic-bound forms. J Mol Biol 405: 173-184.
39. Fedarovich A, Nicholas RA, Davies C (2010) Unusual conformation of the SxN motif in the crystal structure of penicillin-binding protein A from Mycobacterium tuberculosis. J Mol Biol 398: 54-65.
40. Pares S, Mouz N, Petillot Y, Hakenbeck R, Dideberg O (1996) X-ray structure of *Streptococcus pneumoniae* PBP2x, a primary penicillin target enzyme. Nat Struct Biol 3: 284-289.
41. Contreras-Martel C, Dahout-Gonzalez C, Martins Ados S, Kotnik M, Dessen A (2009) PBP active site flexibility as the key mechanism for beta-lactam resistance in pneumococci. J Mol Biol 387: 899-909.
42. Lim D, Strynadka NC (2002) Structural basis for the beta lactam resistance of PBP2a from methicillin-resistant *Staphylococcus aureus*. Nat Struct Biol 9: 870-876.
43. Nicola G, Peddi S, Stefanova M, Nicholas RA, Gutheil WG, et al. (2005) Crystal structure of *Escherichia coli* penicillin-binding protein 5 bound to a tripeptide boronic acid inhibitor: a role for Ser-110 in deacylation. Biochemistry 44: 8207-8217.
44. Dzhekieva L, Rocaboy M, Kerff F, Charlier P, Sauvage E, et al. (2010) Crystal structure of a complex between the Actinomadura R39 DD-peptidase and a peptidoglycan-mimetic boronate inhibitor: interpretation of a transition state analogue in terms of catalytic mechanism. Biochemistry 49: 6411-6419.
45. Sauvage E, Duez C, Herman R, Kerff F, Petrella S, et al. (2007) Crystal Structure of the *Bacillus subtilis* Penicillin-binding Protein 4a, and its Complex with a Peptidoglycan Mimetic Peptide. J Mol Biol.
46. Taschner PE, Ypenburg N, Spratt BG, Woldringh CL (1988) An amino acid substitution in penicillin-binding protein 3 creates pointed polar caps in Escherichia coli. J Bacteriol 170: 4828-4837.

47. Chen Y, Zhang W, Shi Q, Hesek D, Lee M, et al. (2009) Crystal structures of penicillin-binding protein 6 from Escherichia coli. J Am Chem Soc 131: 14345-14354.
48. Kishida H, Unzai S, Roper DI, Lloyd A, Park SY, et al. (2006) Crystal structure of penicillin binding protein 4 (dacB) from *Escherichia coli*, both in the native form and covalently linked to various antibiotics. Biochemistry 45: 783-792.
49. Sung MT, Lai YT, Huang CY, Chou LY, Shih HW, et al. (2009) Crystal structure of the membrane-bound bifunctional transglycosylase PBP1b from Escherichia coli. Proc Natl Acad Sci U S A 106: 8824-8829.
50. Sauvage E, Kerff F, Fonzé E, Herman R, Schoot B, et al. (2002) The 2.4-A crystal structure of the penicillin-resistant penicillin-binding protein PBP5fm from *Enterococcus faecium* in complex with benzylpenicillin. Cell Mol Life Sci 59: 1223-1232.
51. Lovering AL, De Castro L, Strynadka NC (2008) Identification of dynamic structural motifs involved in peptidoglycan glycosyltransfer. J Mol Biol 383: 167-177.
52. Marrec-Fairley M, Piette A, Gallet X, Brasseur R, Hara H, et al. (2000) Differential functionalities of amphiphilic peptide segments of the cell-septation penicillin-binding protein 3 of *Escherichia coli*. Mol Microbiol 37: 1019-1031.
53. Wissel MC, Weiss DS (2004) Genetic analysis of the cell division protein FtsI (PBP3): amino acid substitutions that impair septal localization of FtsI and recruitment of FtsN. J Bacteriol 186: 490-502.
54. Sauvage E, Kerff F, Fonze E, Herman R, Schoot B, et al. (2002) The 2.4-A crystal structure of the penicillin-resistant penicillin-binding protein PBP5fm from Enterococcus faecium in complex with benzylpenicillin. Cell Mol Life Sci 59: 1223-1232.
55. Leimanis S, Hoyez N, Hubert S, Laschet M, Sauvage E, et al. (2006) PBP5 complementation of a PBP3 deficiency in *Enterococcus hirae*. J Bacteriol 188: 6298-6307.
56. Yoshida H, Kawai F, Obayashi E, Akashi S, Roper DI, et al. (2012) Crystal Structures of Penicillin-Binding Protein 3 (PBP3) from Methicillin-Resistant Staphylococcus aureus in the Apo and Cefotaxime-Bound Forms. J Mol Biol 423: 351-364.
57. Romeis T, Holtje JV (1994) Specific interaction of penicillin-binding proteins 3 and 7/8 with soluble lytic transglycosylase in *Escherichia coli*. J Biol Chem 269: 21603-21607.
58. Jennings GT, Savino S, Marchetti E, Arico B, Kast T, et al. (2002) GNA33 from Neisseria meningitidis serogroup B encodes a membrane-bound lytic transglycosylase (MltA). Eur J Biochem 269: 3722-3731.
59. Lovell SC, Davis IW, Arendall WB, 3rd, de Bakker PI, Word JM, et al. (2003) Structure validation by Calpha geometry: phi,psi and Cbeta deviation. Proteins 50: 437-450.

636
637 **Table 1:** Data collection and refinement statistics

| Crystal | $PBP3_{57-577}$ | $PBP3_{88-165}$ SeMet derivative | $PBP3_{88-165}$ |
|---|---|---|---|
| PDB code | 4BJP | | 4BJQ |
| Data Collection: | | | |
| Space group | $P6_122$ | P1 | P1 |
| Cell Dimensions | | | |
| a, b, c (Å) | 119.0, 119.0, 139.2 | 55.8, 55.8, 81.5 | 56.0, 56.0, 82.3 |
| α, β, γ (°) | 90, 90, 120 | 75.8, 89.4, 65.3 | 76.2, 89.1, 66.0 |
| Resolution range (Å)[a] | 82.8 – 2.5 (2.64 – 2.5) | 49 – 2.7 (2.85-2.70) | 38.9 - 2.10 (2.21 – 2.10) |
| No. of unique reflections | 20753 | 45763 | 45669 |
| Rmerge (%)[a] | 16.6 (54.3) | 11.7 (47.8) | 8.0 (50.8) |
| $\langle I \rangle / \langle \sigma I \rangle$ [a] | 13.5 (4.9) | 8.7 (2.6) | 10.2 (2.5) |
| Completeness (%)[a] | 99.8 (98.8) | 95.4 (93.8) | 88.5 (95.4) |
| Redundancy [a] | 14.0 (10.4) | 2.6 (2.6) | 3.7 (3.8) |
| Refinement: | | | |
| Resolution range (Å) | 59.5 - 2.5 | | 35.7 – 2.1 |
| No. of non hydrogen atoms | 3409 | | 5467 |
| Number of water molecules | 135 | | 533 |
| R cryst (%) | 19.9 | | 20.8 |
| R free (%) | 24.5 | | 26.2 |

| | | | |
|---|---|---|---|
| RMS deviations from ideal Stereochemistry | | | |
| Bond lengths (Å) | 0.012 | | 0.010 |
| Bond angles ($^{o}$) | 1.41 | | 1.19 |
| Mean B factor (all atoms) ($Å^2$) | 34.1 | | 31.9 |
| Ramachandran plot [b] | | | |
| Favoured region (%) | 98.5 | | 99.7 |
| Allowed regions (%) | 1.5 | | 0.3 |
| Outlier regions (%) | 0 | | 0 |

[a] Statistics for the highest resolution shell are given in parentheses.

[b] Using program rampage [59]

Figure
Click here to download high resolution image

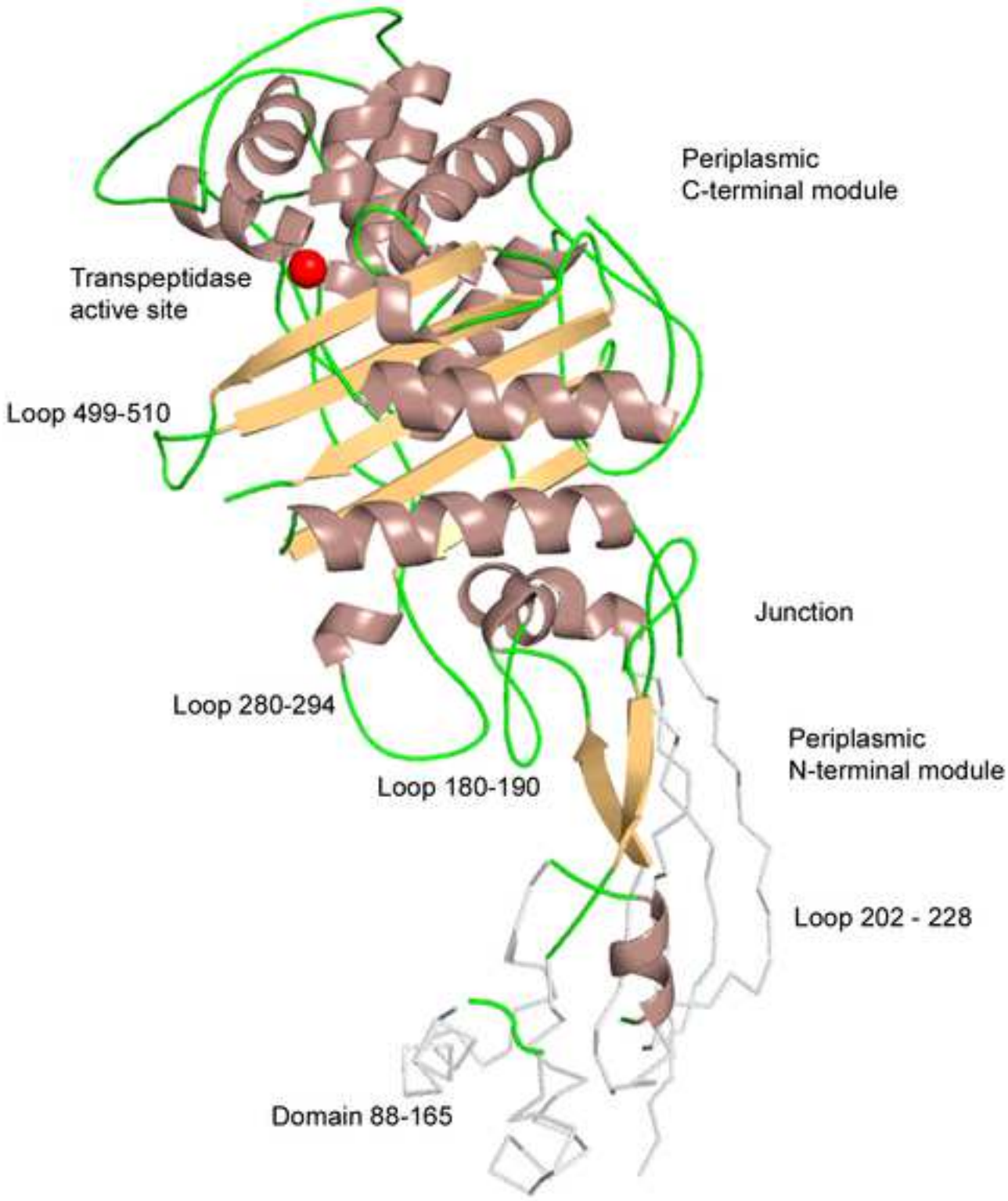

Figure
Click here to download high resolution image

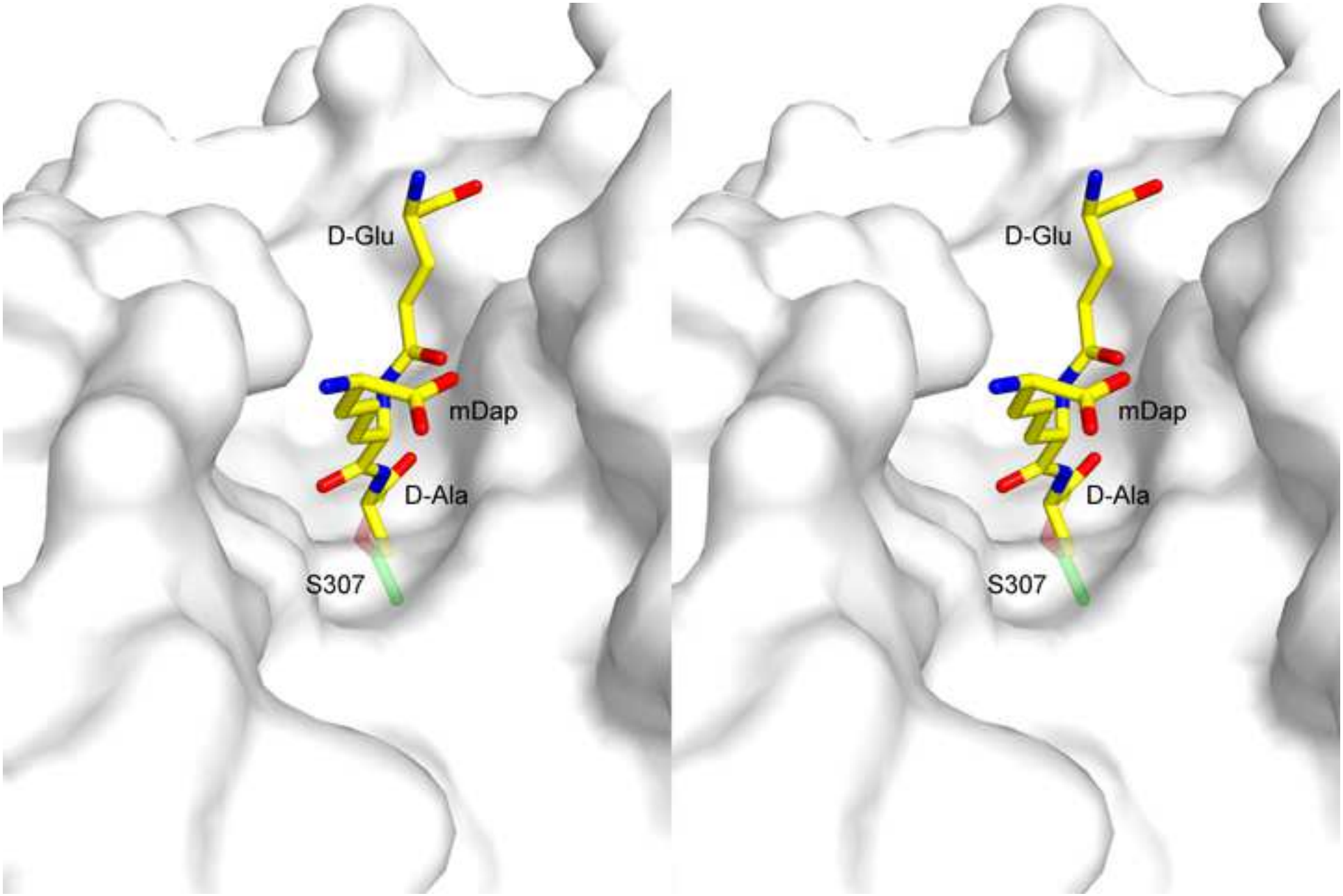

Figure
Click here to download high resolution image

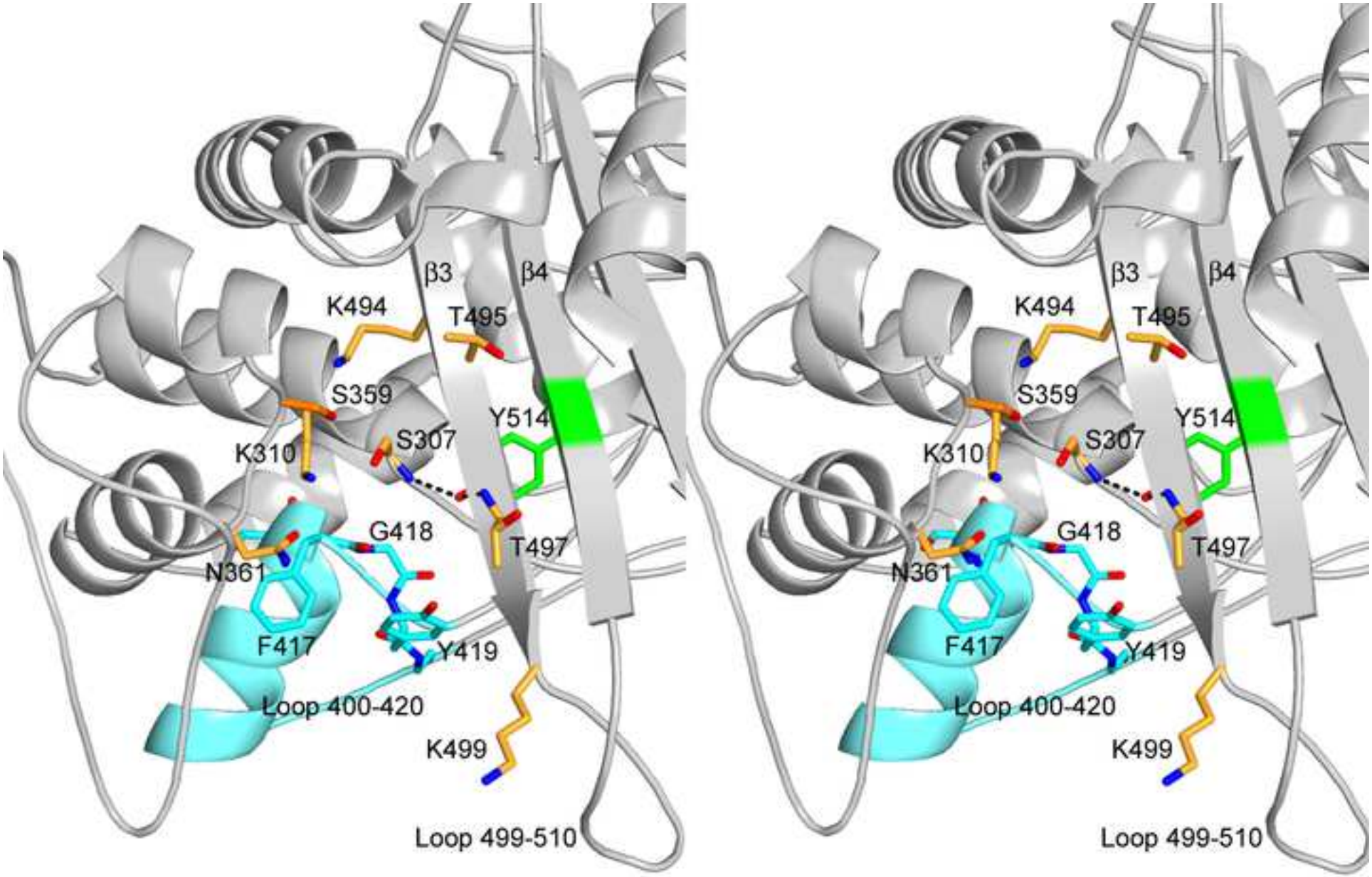

Figure
Click here to download high resolution image

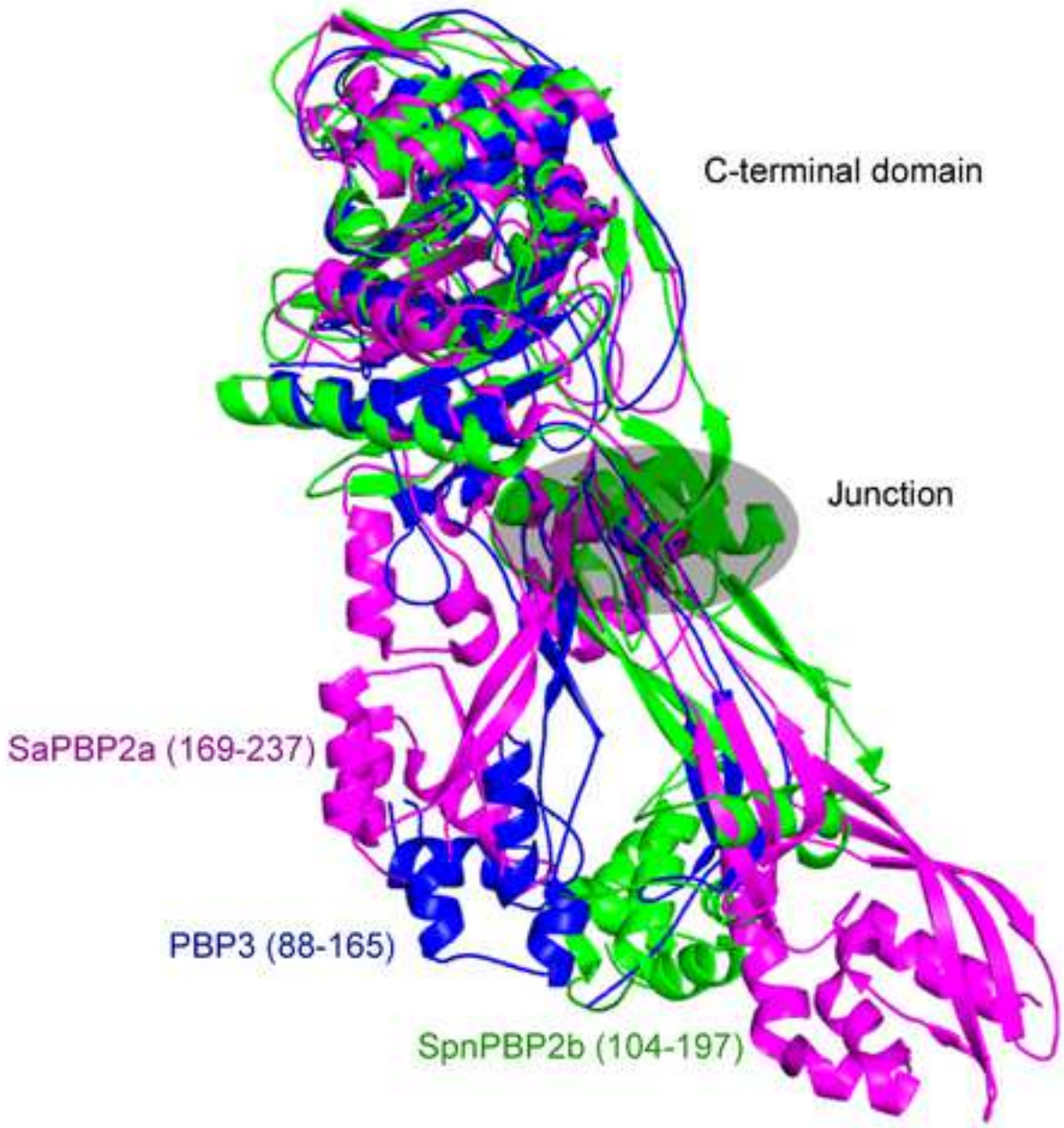

Figure
Click here to download high resolution image

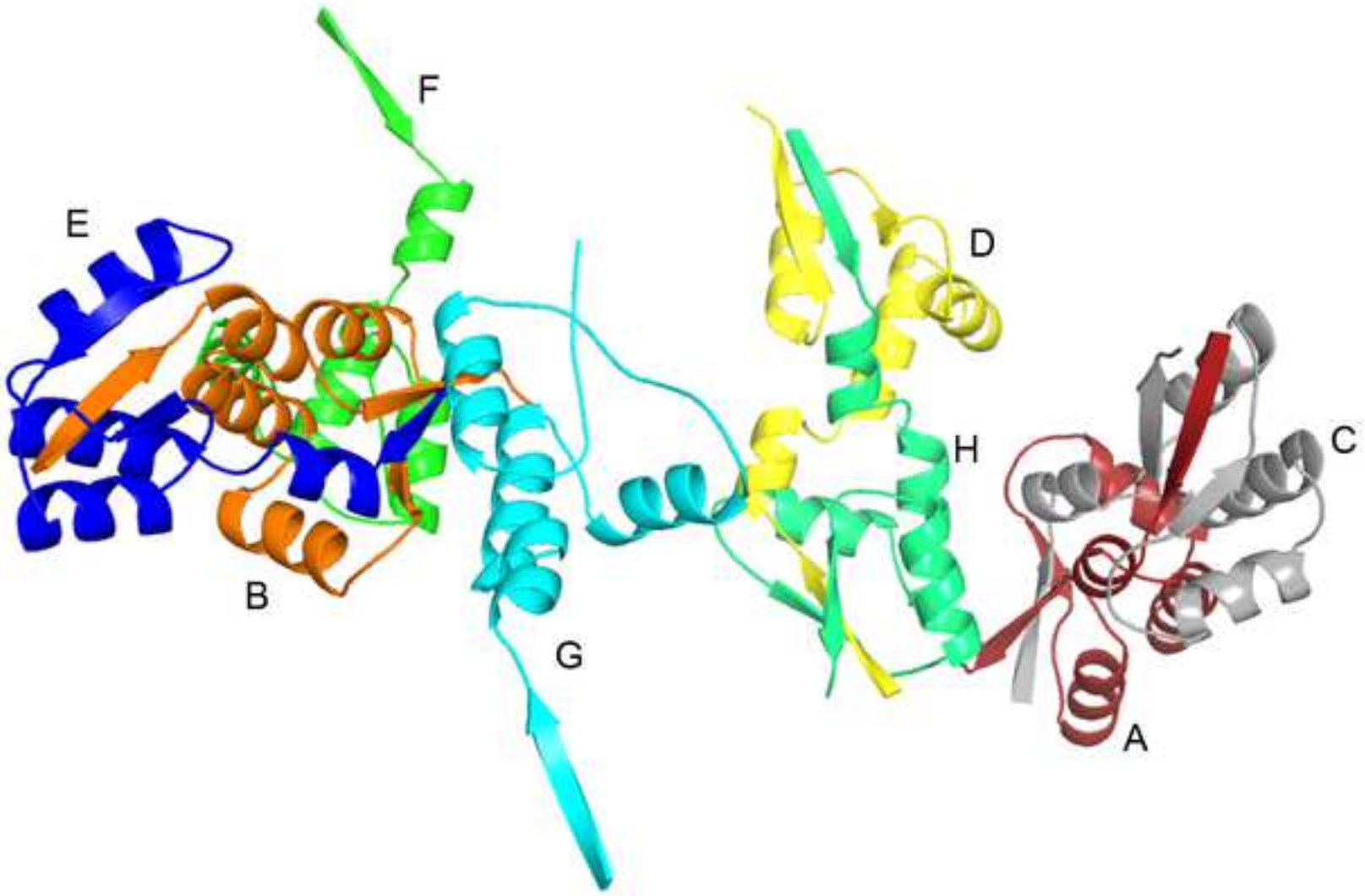

Figure
Click here to download high resolution image

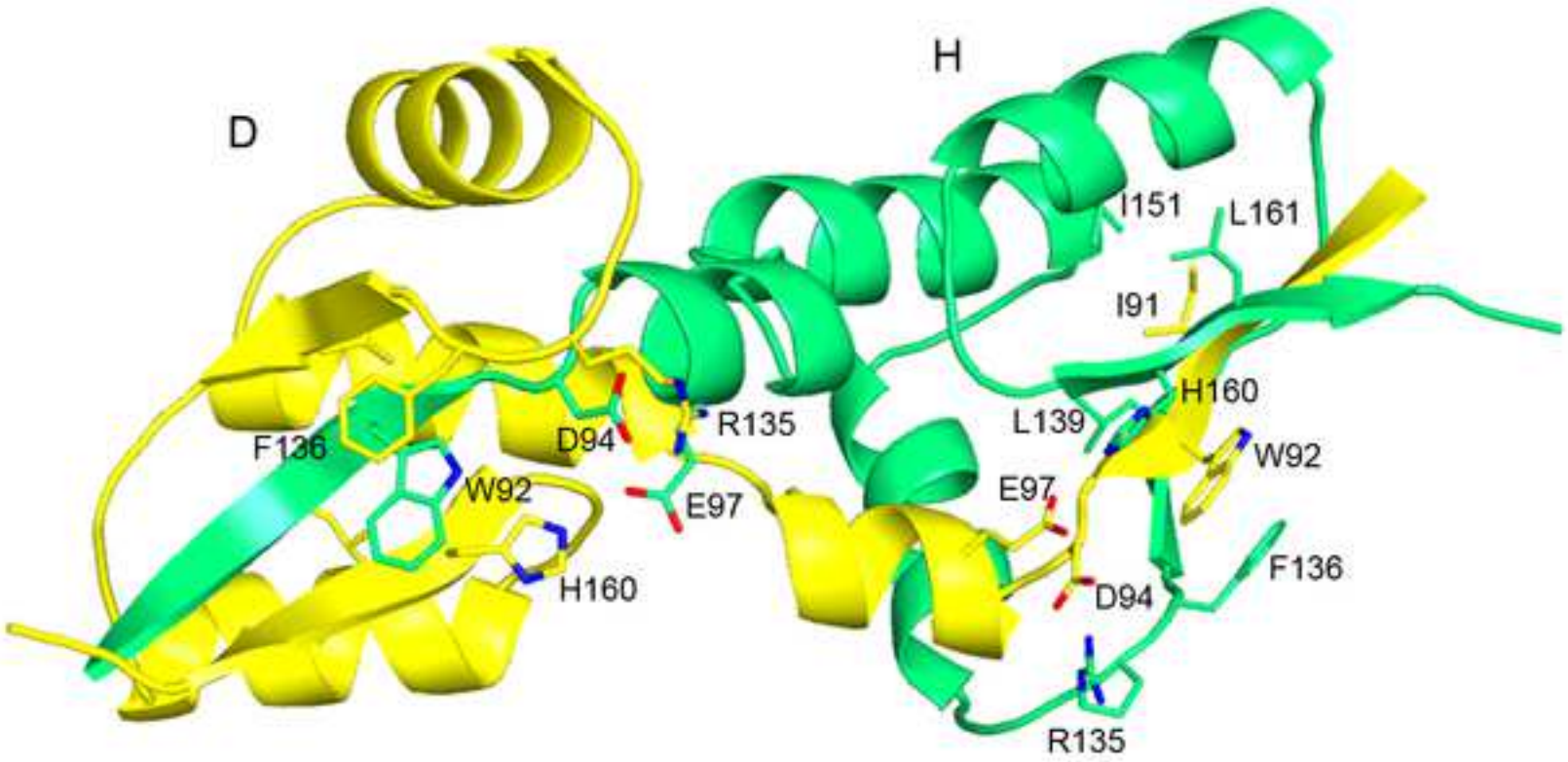

Figure
Click here to download high resolution image

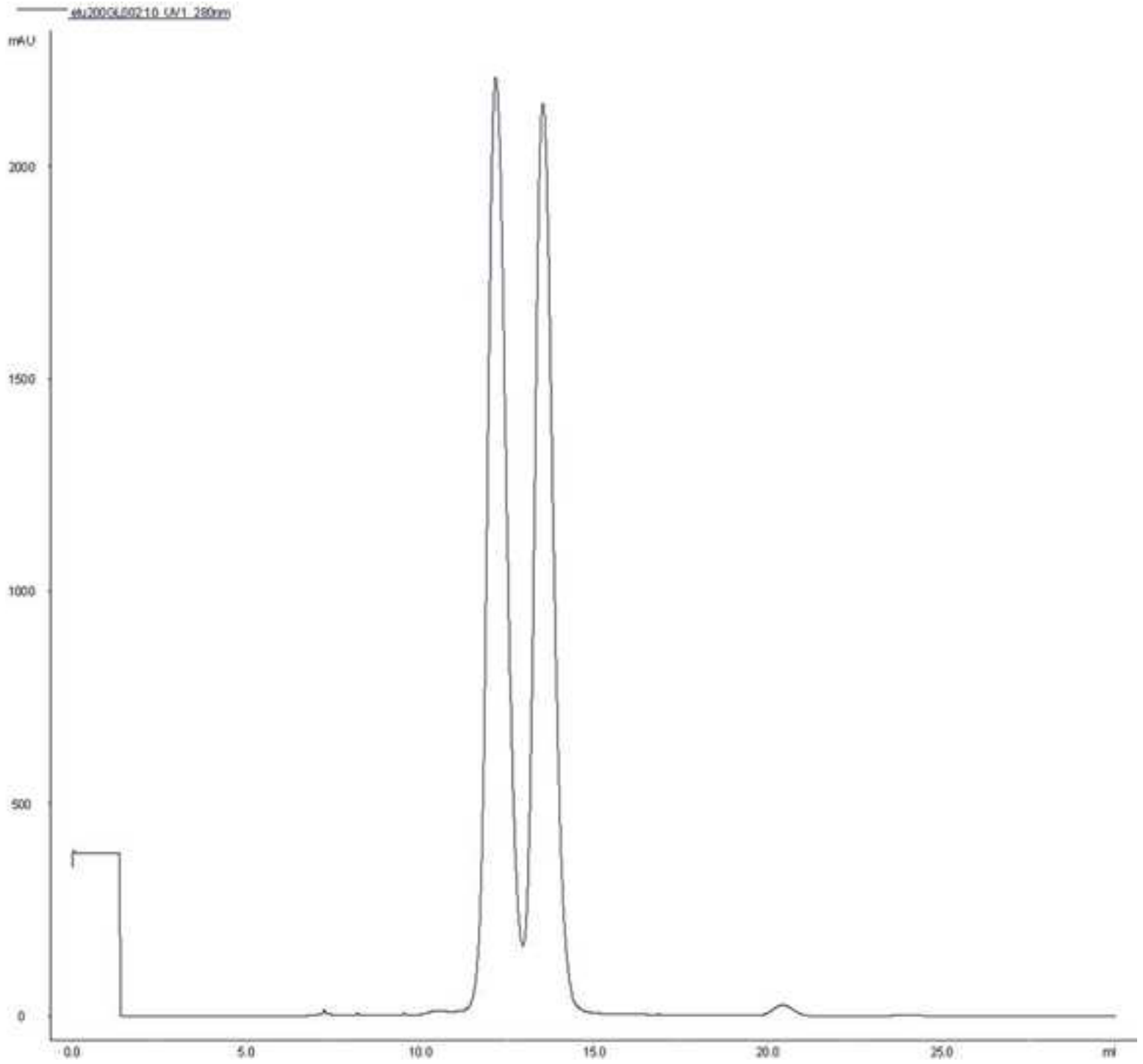

Figure
Click here to download high resolution image

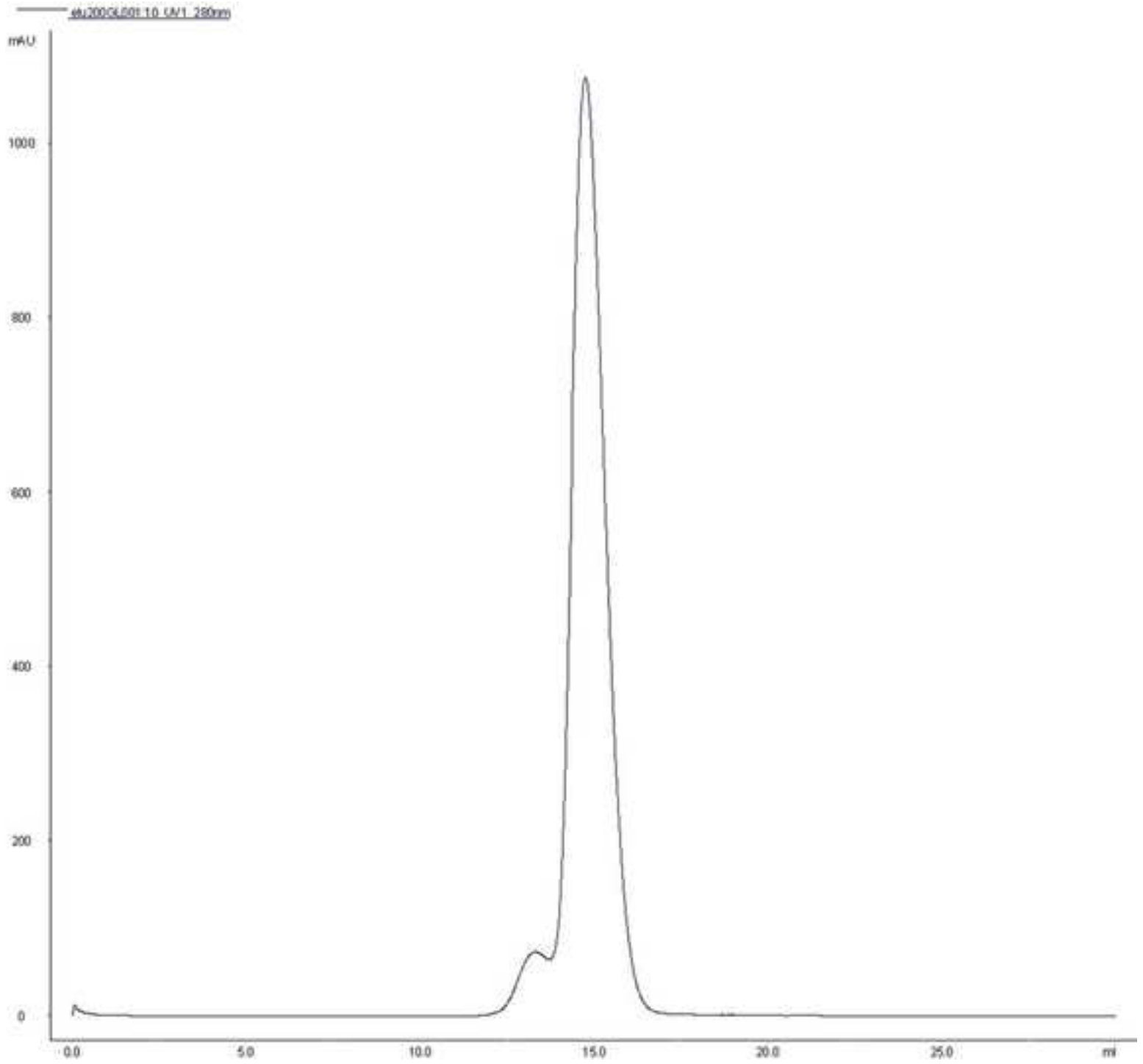

Figure
Click here to download high resolution image

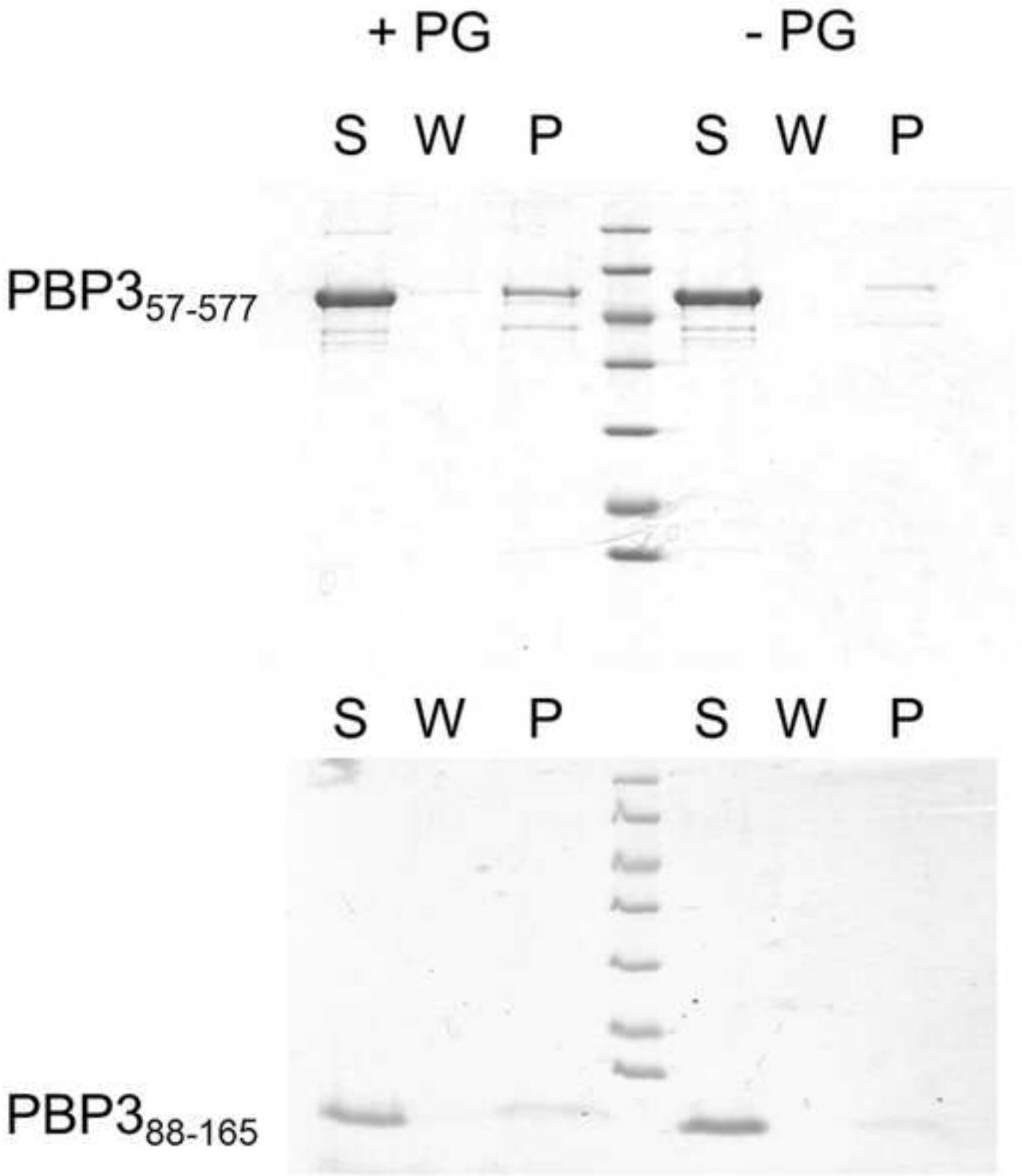

Field Code Changed

# Crystal structure of penicillin-binding protein 3 (PBP3) from *Escherichia coli*

Eric Sauvage [1§]*, Adeline Derouaux [1§], Claudine Fraipont [1], Marine Joris [1], Raphaël Herman [1], Mathieu Rocaboy [1], Marie Schloesser [1], Jacques Dumas [2], Frédéric Kerff [1], Martine Nguyen-Distèche [1] and Paulette Charlier [1].

[1] Centre d'Ingénierie des Protéines, Université de Liège, Institut de Physique B5a et Institut de Chimie B6a, Sart Tilman, B-4000 Liège, Belgium,

[2] Sanofi R&D, protein production, 13 quai Jules Guesde, 94403 Vitry sur Seine, France

Running Title: Structure of *Escherichia coli* PBP3

Corresponding author: Eric Sauvage, Centre d'Ingénierie des Protéines, Université de Liège, Institut de Physique B5, B-4000 Liège, Belgium, Tel: +32 4 366 36 20; Fax: +32 4 366 33 64; E-mail: Eric.Sauvage@ulg.ac.be

§ These two authors contributed equally to the work.

**Abstract**

In *Escherichia coli*, penicillin-binding protein 3 (PBP3), also known as FtsI, is a central component of the divisome, catalyzing cross-linking of the cell wall peptidoglycan during cell division. PBP3 is mainly periplasmic, with a 23 residues cytoplasmic tail and a single transmembrane helix. We have solved the crystal structure of a soluble form of PBP3 ($PBP3_{57-577}$) at 2.5 Å revealing the two modules of high molecular weight class B PBPs, a carboxy terminal module exhibiting transpeptidase activity and an amino terminal module ~~with~~ of unknown function. To gain additional insight, the PBP3 Val88-Ser165 subdomain ($PBP3_{88-165}$), for which the electron density is poorly defined in the PBP3 crystal, was produced and its structure solved by SAD phasing at 2.1 Å. The structure shows a three dimensional domain swapping with a β-strand of one molecule inserted between two strands of the paired molecule, suggesting a possible role in $PBP3_{57-577}$ dimerization.

## Introduction

The penicillin-binding proteins (PBPs) synthesize and remodel the cell wall peptidoglycan, a major component of the bacterial cell wall that gives ~~to~~ the cell its shape and rigidity [1-4]. They are found in all bacteria and represent ~~a~~ major target~~s~~ in anti-biotherapy, especially for the widely used β-lactam antibiotics. Penicillin-binding proteins belong to the family of acyl-serine transferases and are traditionally separated into high-molecular-weight (HMW) PBPs and low-molecular-weight (LMW) PBPs based on molecular weight and sequence homology [4-6]. The former enzymes act as transpeptidases *in vivo* and are involved in ~~direct~~ peptidoglycan synthesis while the latter are carboxypeptidases and endopeptidases [7] thought to remodel peptidoglycan during the bacterial life cycle but details of their *in vivo* ~~activity~~ activities are not well established. The HMW-PBPs group can be subdivided into classes A and B, the LMW group into classes A, B and C. Class B HMW-PBPs can be further divided into subclasses and *Escherichia coli* PBP3 is paradigmatic of subclass B3 that groups class B PBPs from Gram negative bacteria involved in cell division. Some PBPs from Gram positive bacteria involved in spore peptidoglycan synthesis also belong to subclass B3, e.g. SpoVD from *Bacillus subtilis*.

During cell division, the peptidoglycan is synthesized by the periplasmic part of a macromolecular complex called the divisome, made up of at least 20 proteins in *Escherichia coli* [8]. Cell division is initiated by the polymerization of tubulin homolog FtsZ into a contractile ring at midcell [9] and the other division proteins are recruited sequentially to the septal ring. FtsZ first associates with FtsA, ZapA and ZipA that stabilize the FtsZ filaments and tether them to the cytoplasmic membrane. The divisome then matures with a long delay between formation of the Z ring and recruitment of the proteins downstream of FtsK[10]. These proteins involved in septal peptidoglycan synthesis are now thought to be recruited as subcomplexes, at least FtsQ/L/B [11] and FtsW/PBP3 [12]. FtsN, which contains a SPOR

peptidoglycan binding domain, is the last ~~protein~~ essential ~~to~~ division protein that localizes at the septum [13]. Finally, various proteins not essential for septal peptidoglycan synthesis associate with the divisome: the Tol/Pal complex involved in the invagination of the outer membrane [14], and the peptidoglycan hydrolase AmiC (and its activator NlpD) that plays an essential role in the separation of daughter cells ~~separation~~ [15]. Recently, the outer membrane protein ~~Lpob~~ LpoB was also shown to associate with the divisome and to regulate peptidoglycan synthesis by interacting with the glycan chain polymerase/transpeptidase PBP1b [16].

In *E. coli*, PBP3 (FtsI) is an essential protein of the divisome, catalyzing peptide cross-bridges between the glycan chains of the peptidoglycan. PBP3 is involved in many interactions within the divisome. It interacts directly with PBP1b which localizes at the division site during septation in a PBP3 dependent fashion [17]. PBP3 works in concert with PBP1b to incorporate the nascent glycan chain into the existing peptidoglycan [4]. The N-terminal 56 ~~amino acid~~ residues of PBP3 (containing a cytoplasmic peptide, the transmembrane segment and a short periplasmic peptide) interact with PBP1b in a two-hybrid assay. However other interacting sites should be present in the periplasmic part of PBP1b and PBP3 [17]. PBP3 also interacts directly with FtsW and with FtsN, which itself interacts with PBP1b and stimulates its activity [18]. These proteins are able to form a discrete complex independently of the other cell division proteins [12]. Interaction of PBP3 with FtsA, FtsK, FtsQ [19] or FtsL [20] were also reported but the structural details and the sites of interaction between PBP3 and the proteins of the divisome remain to be elucidated.

The *ftsI* gene encodes a 588 residues protein ~~of 588 amino acids~~ but proteolytic cleavage removes 11 amino acids at the C-terminal part of the protein[21]. We have solved the crystal structure of the periplasmic domain of PBP3 (residues 57-577) at 2.5 Å. We have also produced, purified, crystallized and solved the structure of the Val88-Ser165 subdomain

(PBP3$_{88-165}$), a potential protein-protein interaction domain, which was poorly defined in the electron density map of PBP3$_{57-577}$.

## Material and Methods

**Bacterial strains, oligonucleotides and media:** Bacterial strains were *E. coli* Top 10F' for cloning (Invitrogen, USA) and *E. coli* C41(DE3) for expression [22]. Oligonucleotides were from Eurogentec. The rich media used were 2XYT (bacto-tryptone 16 g, yeast extract 10 g, NaCl 5 g, water 1 l, pH 7.0.) or Luria-Bertani (LB) medium supplemented with ampicillin (100 µg ml$^{-1}$), chloramphenicol (20 or 30 µg ml$^{-1}$), kanamycin (50 µg ml$^{-1)}$ and IPTG (0.5 mM) when appropriate.

**PBP3$_{57-577}$: Production, purification, crystallization, data collection and structure refinement.**

Plasmids used were pDML232 for the PBP3 and pDML237 for SecB-[23]~~[12]~~. Fermentation of *E. coli* strain W3110M was performed in RFB MIL11/03 at 37°C to over-express the PBP3(57-577), allowing to obtain soluble protein expression at 210 mg/l~~Litre~~ of culture.

50 g of wet bacterial pellet corresponding to 1 litre of culture were suspended into 150 ml of 100 mM Tris (pH 8), 0.1 mM PMSF buffer, under magnetic stirring in an ice batch for 30 minutes. Mechanical lysis of ~~Bacteria~~ bacteria was performed with a Rannie at 650 bars and cooling. Cell lysate was centrifuged on a JOUAN SR 20.22 at 42 000 g for 1 hour at 4°C. We then centrifuged the supernatant on a Beckman XL90 at 100 000 g for 30 minutes at 4°C, in order to clarify the solution.

The clarified supernatant was loaded on a S-Sepharose Fast Flow column (XK50/30) equilibrated with ~~a~~ buffer A (100 mM Tris (pH 8), 10% glycerol, 10% ethylene glycol) at ~~10~~

Formatted: English (U.S.)

Formatted: English (U.S.)

Field Code Changed

~~ml/min (~~608 ml/h~~31 ch/h)~~. Elution was performed with a linear gradient from 100% of buffer A to 40% of buffer B (buffer A + 1 M Nacl). PBP3 was elu~~a~~ted at about 20% of buffer B. Eluate was diluted 1/3 in buffer A and~~.~~

~~The eluate was then~~ loaded on an S-Sepharose Hiload (XK16/10) column equilibrated in buffer A at ~~30 ch/h~~588 ml/h. Elution was performed with buffer C (100 mM Tris (pH 8), 10% glycerol, 10% ethylene glycol, 0.5 M NaCl). The eluate collected in one column volume was then purified on a Superdex 200 (XK50/60) column at ~~15 cm/h~~294 ml/h to obtain a highly purified and homogenous protein. 120 mg of purified protein were obtained at 1.6 mg/ml (UV measurement). N-terminal sequence was checked and confirmed. Circular dichroism analyses showed that the protein has a stable three-dimensional structure with 30% of alpha-helix. ~~N-terminal sequence was checked and circular dichroism of the aromatic region showed that the protein has a stable three-dimensional environment with 30% of alpha-helix.~~ The FRET (resonance energy transfer) measurements showed a rotational coefficient of 38 ns which demonstrated the monodisperse status of the population with an apparent molecular weight of 53 KDa.

Crystals of $PBP3_{57\text{-}577}$ were grown at 20°C by hanging drop vapor diffusion. Crystals were obtained by mixing 5 µl of a 18 mg~~/~~-ml$^{-1}$ protein solution (also containing 0.5 M NaCl and 20 mM Tris, pH 8), 4 µl of well solution (2.5 M ammonium sulfate and 0.1 M N-cyclohexyl-3-aminopropanesulfonic acid (CAPS), pH 10), and 1 µl of 0.1 M NaCl solution. Crystals appeared after several months and ~~could not be reproduced despite countless attempts.~~ the apparent very narrow range of crystallization conditions resulted in only some very small badly diffracting crystals and one crystal diffracting at 2.5 Å. Diffraction data were measured on Beamline ID29 at the European Synchrotron Radiation Facility (ESRF, Grenoble, France) and processed using Mosflm [24] and SCALA from the CCP4 program suite. [25] The structure of PBP3 was solved by molecular replacement with the program PHASER [26]

using the structure of PBP2 from *Neisseria gonorrhoeae* (PDB id: 3equ) as the initial search model. Refinement was carried out using REFMAC5, [27] TLS, [28] and Coot. [29]. The final refinement statistics are given in Table 1.

**PBP3$_{88-165}$: Production, purification, crystallization, data collection and structure refinement.**

The *ftsI* fragment encoding PBP3$_{88-165}$ was amplified by PCR using plasmid pMVRI [17] as template and oligonucleotides 5'-GGACCCGGGGTAAAAGCGATTTGGGCTGACCC-3' and 5'-GCCGGATCCTTAAGAC TCTTCACGCAGATGAATCCC-3' as primers (*XmaI* and *BamHI* are underlined). The PCR fragment was cloned into the pJet1.2/blunt cloning vector (Fermentas), sequenced, digested with *XmaI* and *BamHI* and inserted into the same sites of plasmid pET-52b(+). The resulting plasmid pDML2042 codes for the PBP3$_{88-165}$ with an N-terminal strep-tag. The strep-tag- PBP3$_{88-165}$ was isolated from *E. coli* C41(DE3) harbouring pDML2042 grown at 37° C in 2XYT medium in the presence of 0.5 mM IPTG for 3h. The harvested cells were suspended in 40 ml of 100 mM Tris-HCl pH 8.0, 150 mM NaCl, 1mM EDTA containing a~~n~~ protease inhibitor cocktail ~~protease~~ (Roche) (buffer C), broken 5 times into a high-pressure homogenizer (Emulsiflex-C3 Avestin Inc.) and centrifuged at 25000g for 40 min. The supernatant was filtered (0.45µ) and applied to a 5 ml *Strep*-Tactin ~~column~~ IBA column. After 5 washes with buffer C, the strep-tag-PBP3$_{88-165}$ was eluted in 100 mM Tris-HCl pH8.0, 150 mM NaCl, 1mM EDTA, 2.5mM desthiobiotin. The fractions of interest (5ml) were dialyzed against 2 L of buffer C with a 3,500 Dalton cut off membrane and analyzed ~~on~~ by SDS-18% PAGE. About 6 mg of PBP3$_{88-165}$ per liter of culture ~~was~~ were produced and purified to 90% purity. The strep-tag was removed from PBP3$_{88-165}$ before crystallization.

Crystals of PBP3$_{88-165}$ were grown at 20°C by hanging drop vapor diffusion. Crystals were obtained by mixing 4 µl of a 7.5 mg~~/~~ml$^{-1}$ protein solution containing 0.15 M NaCl and 0.1 M

Tris, pH 8 1mM EDTA, and 1 µl of well solution (2 M ammonium sulfate and 0.1 M citrate, pH 3.5). The structure of $PBP3_{88-165}$ was solved by single anomalous diffraction using a selenomethionine substituted $SePBP3_{88-165}$ crystal. Selenomethionine substituted $SePBP3_{88-165}$ was expressed by using minimal medium supplemented with selenomethionine and purified and crystallized as $PBP3_{88-165}$. Diffraction data for the $SePBP3_{88-165}$ crystals were measured on Beamline PROXIMA 1 at SOLEIL (Paris, France). Data were processed using XDS [30] and initial structure determination of $SePBP3_{88-165}$ was determined with the help of SHELXC/D/E [31], Parrott [32] and Buccaneer [33].

Refinement was carried out on native $PBP3_{88-165}$ using REFMAC5, [27] TLS, [28] and Coot. [29]. Diffraction data for the native $PBP3_{88-165}$ were measured on Beamline BM30A at the European Synchrotron Radiation Facility (ESRF, Grenoble, France) and processed using Mosflm [24] and SCALA from the CCP4 program suite. [25] Data and final refinement statistics are given in Table 1.

**Western blotting:** Western blotting was carried out as described [12]. PBP3, PBP1b and FtsN were revealed with respective polyclonal antibodies and FtsW was probed with monoclonal anti-HA-Peroxydase (HighAffinity (3F10) Roche).

.

**Light Scattering (DLS and SLS).**

Dynamic and static light scattering data were recorded on a DynaPro NanoStar instrument (Wyatt Technology Corporation) operated in batch mode at 20°C and fitted with a laser beam emitting at 658 nm with power auto-attenuation. Scattering angles were 90° for both DLS (avalanche photodiode) and SLS (silicon PIN photodetector). Measurements were performed under buffer conditions and concentration used for crystallogenesis. Samples were filtered on Whatman Anotop 10 inorganic membrane (0.02 µm cut off) and loaded into a 10 µl quartz

Field Code Changed
Field Code Changed
Field Code Changed
Field Code Changed

microcuvette. Data were averaged from 20 acquisitions of the scattered light intensity during 5 s, with a sum of squares error value below 100. Scattering data were analyzed using DYNAMICS v. 7.1.1.3 software (Wyatt Technology Corp.) that includes the DYNALS module for distribution analysis in photon correlation spectroscopy. A globular protein model was used for mass estimation in DLS and a dn/dc value of 0.185 m~~L~~l/g for mass calculations in SLS. Theoretical protein hydrodynamic radii were calculated from pdb files with program HYDROPRO [34].

**Protein binding to peptidoglycan.** Protein binding to peptidoglycan was ~~realized~~ performed as described in Typas *et al.* [16]. Briefly, 10 µg of protein ~~was~~ were incubated with a peptidoglycan suspension of *E. coli* MC1061. The peptidoglycan was pelleted, washed and resuspended in 2% SDS. The unbound fraction, the wash fraction and the resuspended pellet were ~~loaded on~~analysed by SDS-18% PAGE. A control sample was realized without peptidoglycan.

**Gel filtration.** Gel filtration experiments were performed on a Superdex 200 10/300 GL and on a Superdex 75 10/300 GL for $PBP3_{57-577}$ and $PBP3_{88-165}$ respectively. The proteins were used at the same concentration and in the same buffer as in the crystallogenesis assay and in DLS. 200 µl of protein were injected. Standard proteins (lysozyme 14.3 ~~K~~kDa, trypsin inhibitor 20.1 k~~K~~Da, carbonic anhydrase 31 k~~K~~Da, bovine serum albumin 66.5 k~~K~~Da) were used for calibration.

**Accession numbers.** The atomic coordinates for the crystal structure of $PBP3_{57-577}$ and $PBP3_{88-165}$ are available at the Protein Data Bank with the accession numbers PDB ID: **4BJP** and **4BJQ**.

## Results and discussion

### Structure determination

The crystal structure of a soluble form of PBP3, including residues 57 to 577, was solved at 2.5 Å resolution. The structure of PBP3 was solved by molecular replacement using the structure of PBP2 from ~~*Neisseria* *N.*~~ *gonorrhoeae* (PDB id: 3equ) [35]. PBP3 crystallizes in space group $P6_122$ with one molecule in the asymmetric unit. The structure was built from residues 71 to 567 but absence of detectable electronic density did not allow structure determination for residues 93-112, 119-141, 152-162, 202-228 and 537-543. PBP3 structural information ~~have been~~was supplemented by independently solving the Val88-Ser165 subdomain structure (see below). Final $R_{cryst}$ and $R_{free}$ values for the PBP3 structure determination are 19.9 % and 24.5 % respectively.

The overall fold of periplasmic PBP3 is bimodular (Fig. 1~~a~~). The C-terminal module is~~,~~ responsible for the transpeptidase activity~~, is associated to~~ but no clear function has been assigned yet to the N-terminal module of the construct~~, for which no clear function has been assigned yet~~.

~~.~~

### Transpeptidase module and active site

The C-terminal module shares its overall fold with the transpeptidase domain found in all PBPs [5,36]. Structure-based alignments of the PBP3 transpeptidase domain show little structural deviations from the corresponding domains of class B3 PBPs with r.m.s.deviations of 1.3 Å (Acitenobacter baumanii PBP3 [37]), 1.3 Å (*Pseudomonas aeruginosa* PBP3 [38] and 1.4 Å (*N.gonorrhoeae* PBP2 [35] and larger deviations for class B PBPs from other subgroups (1.7 Å, 2.1 Å, 2.1 Å, and 2.1 Å for *Mycobacterium tuberculosis* PBPA [39], *Streptococcus pneumoniae* PBP2x [40], *S. pneumoniae* PBP2b [41] and *Staphylococcus aureus* PBP2a [42], respectively). The active site responsible for the transpeptidase activity of

PBP3 is located in a long groove that can accommodate the carboxy-terminal residues of the PBP3 natural substrate, the peptidoglycan stem pentapeptide L-Ala-γ-D-Glu-meso-diaminopimelic acid (mDAP)-D-Ala-D-Ala (Fig 2a).

The transpeptidase activity of PBP3 ~~depends upon~~relies on eight residues, Ser307, Lys310, Ser359, Asn361, Lys494, Thr495, Gly496 and Thr497, found with few exceptions in all penicillin-binding enzymes (Fig. 2~~1~~b). These residues form three conserved sequence motifs (Ser-Xaa-Xaa-Lys, Ser-Xaa-Asn and Lys-Thr-Gly-Thr) and are also responsible for the binding of β-lactam antibiotics to the active site of PBPs [5].

The mechanism leading to linkage between the stem peptides of two glycan chains involves an acyl-enzyme formed between the active serine and the penultimate D-Ala of one stem peptide, releasing the ultimate D-Ala. In this mechanism, the nucleophylicity of the active serine Ser307 would be enhanced by Lys310, and Ser359 would be important for back-donation of the proton to the active serine during the acylation step. Deacylation involves the attack of the acyl bond by the free amine group of a second stem peptide diaminopimelic acid. Lys494 could play an important role in deacylation in concert with Ser359, as suggested for other PBPs [43-45].

Asn361 should be important for proper positioning of the interpeptidic amide group linking the penultimate D-Ala to the diaminopimelic acid residue. Substitution of Asn361 by a serine causes a dramatic change in pole shape [46]. The pointed polar caps observed in the *E. coli* mutant harboring this mutation appeared to be associated with the activity of PBP3. Asn361 differentiates PBP3 from its elongation homologue PBP2. The presence of an aspartic acid at this position in *E. coli* PBP2 and more generally in all PBPs of class B2(~~,~~ which contains Gram negative class B PBPs associated to elongation~~,~~) is a noticeable exception to the conservation of this residue in peptidoglycan synthesizing PBPs. The nature of the amino-acid should be of importance for the fine structural conformation of peptidoglycan.

Finally, both threonine residues of the Lys-Thr-Gly-Thr motif should serve as an anchor to the C-terminal carboxylate group of the pentapeptide. They are found hydrogen bonded to the penultimate D-Ala carboxylate in structures of DD-peptidases in complex with peptide fragments [45,47].

In all ligand-free PBP-structures a water molecule is observed in the oxyanion hole. In PBP3, the oxyanion hole, defined by the amine groups of residues 307 and 497, is unexpectedly occupied by the hydroxyl group of Tyr514 that is ~~distant by~~at 2.7 Å from Ser307N and 3.25 Å from Thr497N (Fig. ~~1b~~2b). Sequence alignment shows that Tyr514 is unique to PBP3 among class B PBPs. The side chain of Tyr514 is free to easily rotate and liberate the oxyanion hole and should not play a particular role in transpeptidation.

The rear side of the PBP3 active site is made of residues Phe417-Gly-Tyr-Gly (Fig. ~~1b~~2b). The motif Tyr/Phe/Ile-Gly-Tyr/Gln-Gly and the ~~conformation~~ tertiary structure of the segment 402-420 are conserved in each class of ~~all~~ PBPs. Gly418 closes a hydrophobic pocket that can accommodate the methyl group of the penultimate D-alanine of the stem pentapeptide, conferring to PBPs a high specificity for a D-alanine as the fourth residue of the pentapeptide.

Electron density around residues 499-510, a loop that connects ~~two~~ strands β3 and β4 close to the active site, is weak but sufficient to allow its determination. Disorder of this loop is a general property of class B PBPs whereas in other classes of PBPs, a small hairpin connects the two strands [38,43,47-50]. It could be stabilized by interactions with another protein of the divisome, e.g. for an adequate position and orientation of the active site of PBP3 along with the transpeptidase active site of PBP1b. The loop could also have a role for accompanying the displacement of the glycan chain on the surface of PBP3. In a similar manner, a disordered loop in the glycosyltransferase domain of ~~*Staphylococcus*~~ *S. aureus* PBP2, a class A PBP

homologous to PBP1b, was proposed to allow the nascent glycan chain to move processively from the donor site to the acceptor site [51].

**N-terminal module**

The N-terminal module provides three loops (180-190; 202-228; 280-294) and one subdomain (88-165) for potentially interacting with other proteins of the divisome. The residues between these loops and subdomain form a series of motifs well conserved in the primary sequence of class B PBPs [4], forming the junction between the C- and N-terminal modules and tethering the loops from the latter to the C-terminal module. Comparison with the structures of other class B PBPs shows that the relative position between the two modules can vary, ~~provides evidence~~suggesting that the junction between both modules is flexible. Difference between apo and acyl-enzyme structures of *P. aeruginosa* PBP3 led to the same conclusion [38]. Figure 3 shows the structures of *S. aureus* PBP2a [42] and *S. pneumoniae* PBP2b [41], with their C-terminal domain superposed onto that of PBP3, highlighting the fact that the domains equivalent to $PBP3_{88\text{-}165}$ (domain 169-237 for SauPBP2a and domain 104-197 for SpnPBP2b) lie in different position. Class A PBPs also show a high degree of flexibility between their glycosyltansferase module and the ensemble made of the linker and the transpeptidase module [51]. Such flexibility could be necessary for the enzyme to reach its target or be required for ~~a processive~~ displacement of the divisome along the septum.

The 180-190 loop forms a small β-hairpin exposing Val184 and Asp185 to the solvent. The length of this loop is characteristic of class B PBPs pertaining to the divisome (PBP3) and is much longer in class B PBPs acting during elongation (PBP2). The 280-294 loop, from the C-terminal module, is close to the 180-190 loop and is also longer in the PBPs of the elongation complex than in the PBPs of the divisome. These two loops could thus represent a specific PBP3 zone of interaction with partners of the divisome, preventing PBP3 to associate with

**Formatted:** Font: Italic
**Formatted:** Font: Italic
**Formatted:** Font: Italic
**Formatted:** Font: Italic

proteins of the elongation complex or, conversely, preventing PBP2 to associate with proteins of the divisome.

Electron density is absent for segment 202-228, which again suggests that interactions with a partner protein may stabilize its tertiary structure in the divisome. Marrec-Ffairley *et al.* [52] have characterized mutants of the E206-V217 segment consistent with such a role in protein interaction. R210 seems particularly important, together with residues G57, S61 and L62, for the recruitment of FtsN [53].

**PBP3$_{88\text{-}165}$ subdomain**

Electron density was very poor for residues between Val88 and Ser185, with only some secondary structures showing up in the electron density maps. Apparent disorder of domain 88-165 is also observed in ~~*Neisseria*~~ *N. gonorrhoeae* PBP2 [35] and to a lesser extent in *Pseudomonas aeruginosa* PBP3 [38], ~~*Acetinobacter*~~ *Acinetobacter Baumanii* PBP3 [37], *Enterococcus faecium* PBP5 [54] and ~~*Streptococcus*~~ *S. pneumoniae* PBP2x [40], all of which are class B PBPs. Interaction of this domain with another protein of the divisome may stabilize its tertiary structure. In order to determine its three-~~ri~~dimensional structure, the PBP3$_{88\text{-}165}$ domain was produced and its structure solved.

The domain crystallizes in P1 with eight molecules in the asymmetric unit. Because of the high number of copies in the asymmetric unit, molecular replacement using the closely related domain Val79-Phe151 of *P. aeruginosa* PBP3 failed to provide a solution, whatever the Molecular Replacement program used. The structure of the PBP3$_{88\text{-}165}$ domain was eventually determined by single anomalous diffraction using a selenomethionine substituted PBP3$_{88\text{-}165}$ crystal and refined over data collected on a crystal of the native PBP3$_{88\text{-}165}$ protein. The electron density is well defined except for residues 132-135 in chain F and for the C-terminal residue in chains E, G and H. Final Rwork and Rfree values for the PBP3$_{88\text{-}165}$ domain are

20.9 % and 26.3 % respectively. The eight molecules in the asymmetric unit are organized in four pairs with, in each pair, 18 N-terminal residues swapping into the paired molecule (~~Figure~~ Fig. ~~2a~~4a). The swapped residues represent a two-turn helix and a β-strand that inserts between two β-strands of the other molecule to form a three stranded β-sheet. Interactions between the two molecules are numerous and include many hydrogen bonds, salt bridges (e.g. for associated chains A and C: Asp94A-Arg135C, Glu97A-His160C), hydrophobic clusters (Ile91A is surrounded by seven leucines or isoleucines from chain C), and an aromatic ring stacking (Trp92A is sandwiched between Phe136C and His160C) (~~Figure~~ Fig. ~~2b~~4b). Together, residues 88-105 from one molecule and residues 106-165 from the paired molecule form a small globular domain whose tertiary structure, three anti-parallel β-strands flanked by three helices, is homologous to the equivalent domain of *P. aeruginosa* PBP3.

Mutations in the *E. hirae* $PBP5_{190\text{-}261}$ domain, homologous to $PBP3_{88\text{-}165}$, ~~have accredited~~support the hypothesis that this domain is a good candidate to play a role in protein-protein interactions [55]. Of note is the insertion of 60 residues assembling in four helices in the corresponding domain of PBPs of subclass B5 [41,56].

**PBP3 dimers.**

PBP3 dimerization was shown *in vivo* by two-hybrid assay [19,20] and FRET [12], and the structure of $PBP3_{88\text{-}157}$ suggests that PBP3 dimerization could be reinforced by 3D domain swapping involving residues 88-105. The weak electronic density around domain 88-165 in the crystal of $PBP3_{57\text{-}577}$ allows the approximate positioning of $PBP3_{88\text{-}165}$ structure in the crystal of $PBP3_{57\text{-}577}$. $PBP3_{88\text{-}165}$ then faces a symmetric domain with the crystallographic axis of symmetry at the hinge point where domain swapping occurs in $PBP3_{88\text{-}165}$, raising the possibility that swapping also occurs in the crystal of $PBP3_{57\text{-}577}$. Domain swapping in ~~the~~ $PBP3_{57\text{-}577}$ would yet involve a twisting of $PBP3_{88\text{-}165}$ domain, i.e. symmetrical $PBP3_{88\text{-}165}$

domains would not be oriented in the $PBP3_{57-577}$ crystal in the same manner as in the $PBP3_{88-165}$ one.

The oligomerization state of $PBP3_{88-165}$ and $PBP3_{57-577}$ was investigated by Light Scattering and gel filtration. DLS and SLS experiments carried out on a solution of $PBP3_{88-165}$ suggested a dimer in solution. The monodisperse distribution observed in DLS provided a hydrodynamic radius of 18 Å corresponding to the radius of the $PBP3_{88-165}$ dimeric form calculated from the coordinate file whereas the average molecular mass given by SLS was 27 kDa, which is an overestimated mass of $PBP3_{88-165}$ dimer due to the strong influence ~~on mass calculation~~ of small quantities of remaining aggregates on mass calculation. Gel filtration assays carried out with $PBP3_{88-165}$ provided 2 peaks representing each 50% of the total protein content (~~Supplementary figure 1~~Fig. 5a). The second peak represents $PBP3_{88-165}$ dimers and the first peak accounts for higher order multimers. From these results, we conclude that, at the concentration used for crystallization, monomers of $PBP3_{88-165}$ are absent and dimers are predominant in the solution.

DLS analysis of $PBP3_{57-577}$ exhibited unimodal particle-size distributions with an intensity-average hydrodynamic diameter of 48 Å. Hydrodynamic radii calculated from pdb files gives 27 Å and 54 Å for a monomer or a dimer of $PBP3_{57-577}$ respectively, suggesting that a dimer is predominant in solution. This was confirmed by SLS analysis, which provided a molecular mass of 108 kDa, corresponding to a $PBP3_{57-577}$ dimer. In gel filtration assays, $PBP3_{57-577}$ was mainly eluted as a monomer with 5% of dimers (~~Supplementary figure 2~~Fig. 5b), which might be explained by the constant displacement of the equilibrium toward the monomer when it is separated by the size from the dimer. At the concentration used for crystallization, dimers of $PBP3_{57-577}$ can predominate in the solution but monomers are also present and it remains unclear if $PBP3_{57-577}$ dimerization results directly from 3D domain swapping.

3D domain swapping is frequently observed as an artefact resulting from crystallization, without bearing relevance to biological function. Because domain swapping in the $PBP3_{57-577}$ crystal would involve a large twisting of the (88-165) domain and, also, because domain swapping should stabilize the domain and hence provide a clear electronic density in that region, the domain swapping observed in the case of $PBP3_{88-165}$ is probably absent in the $PBP3_{57-577}$ crystal. Moreover, in the full PBP3, domain swapping would extend from residue 105 to the amino terminus and swapping of such a large domain has never been reported. A role for domain swapping in the *in vivo* dimerization of PBP3 seems therefore elusive.

**$PBP3_{88-165}$ interactions**

PBP1b, FtsN or FtsW are known to interact with PBP3 but a direct interaction between these proteins and the $PBP3_{88-165}$ domain could not be detected using affinity chromatography (data not shown). Nevertheless, $PBP3_{88-165}$ *in vitro* dimerization by domain swapping could impair the interaction, if any, of the $PBP3_{88-165}$ domain with one of these proteins and an *in vivo* interaction of the domain with PBP1b, FtsN or FtsW cannot be discarded.

The subcomplex FtsQ/FtsL/FtsB could also be involved in the interaction with $PBP3_{88-165}$. The N-terminal module of PBP3 appears to interact with FtsL in a two-hybrid system [20]. Lytic transglycosylases represent other potential candidates for an interaction with $PBP3_{88-165}$. In *E. coli*, the soluble lytic transglycosylase Slt70 was shown to interact with PBP3 [57], whereas in *N. meningiditis* the membrane bound lytic transglycosylase MltA was shown to interact with PBP2Ng [58], the orthologue of *E. coli* PBP3.

We tested the possibility that the $PBP3_{88-165}$ domain could interact with the peptidoglycan. The binding of $PBP3_{57-577}$ and $PBP3_{88-165}$ to peptidoglycan sacculi was tested by a pull-down assay (~~Supplementary figure 3~~Fig. 6). We showed that a part of $PBP3_{57-577}$, but not $PBP3_{88-165}$, was pelleted with the sacculi indicating that it has an affinity for the peptidoglycan. On the

whole, results indicate that this region of PBP3 is not essential for its interaction with the murein sacculus although $PBP3_{88-165}$ dimerization could also perturb a possible interaction with the peptidoglycan.

## Conclusion

PBP3 interacts with many proteins and occupies a central role in the periplasmic component of the divisome. The structural information brought by the resolution of the PBP3 structure adds to the available structures of *E. coli* PBP1b, FtsQ, and FtsN carboxy terminal domain.

The modular organisation and the non-folded nature of the small loops or subdomains composing the PBP3 N-terminal module suggest that the latter could be involved in protein-protein interactions with partners of the divisome.

The structure of the $PBP3_{88-165}$ domain, disordered in PBP3, shows a dimerization of the domain by three dimensional domain swapping that is possible but unlikely in the full length PBP3. Domain swapping in $PBP3_{88-165}$ domain is unlikely to play a role in the *in vivo* PBP3 dimerization and a role in protein-protein interaction remains the most attractive hypothesis for this small domain.

**Acknowledgments**

We thank Andy Thompson for his help on Beamlines Proxima1 (SOLEIL) and ID29 (ESRF), Jean – Luc Ferrer for his help on BM30a (ESRF), Maxime Lampilas and Joszef Aszodi for their participation in the PBP3 production and Georges Feller for his expertise with SLS/DLS.

~~**Supporting information**~~

~~**Figure S1**: Chromatogram of PBP3$_{88-165}$ gel filtration on a Superdex 75 10/300 GL.~~

~~**Figure S2**: Chromatogram of PBP3$_{57-577}$ gel filtration on a Superdex 200 10/300 GL.~~

~~**Figure S3**. Pulldown of PBP3$_{57-577}$ and PBP3$_{88-165}$ with and without peptidoglycan sacculi.~~

444 **Figure legends**

445

446 ~~**Figure 1 Structure of E. coli PBP3.** (a) View of the crystal structure of PBP3 showing the~~
447 ~~penicillin-binding module in orange and the amino-terminal periplasmic module in blue.~~
448 ~~Modelled loops undefined in the crystal structure are shown in lightblue. The transmembrane~~
449 ~~helix (not in the PBP3 construct) is shown in grey. The active site is indicated by a green~~
450 ~~sphere. The cytoplasmic domain is not shown. Loops discussed in the text are indicated. (b)~~
451 ~~PBP3 transpeptidase active site. Cartoon stick representation of the transpeptidase active site~~
452 ~~of PBP3. Strand delineating the right of the active site is shown in sticks to unhide tyr514~~
453 ~~(green). The oxyanion hole is defined by the nitrogen atoms of residues 307 and 497. Loop~~
454 ~~400-420 is shown in cyan. Nitrogen atoms are shown in blue and oxygen atoms in red.~~

455

456 ~~**Figure 2 Domain swapping in PBP3$_{88-165}$.** (a) PBP3$_{88-165}$ crystal unit cell (space group P1).~~
457 ~~The 8 chains are organized by pairs with 18 swapped residues. (b) Interactions between~~
458 ~~swapped residues from chains D (yellow) and H (green), including the hydrophobic cluster~~
459 ~~around Ile91 (Leu139, Ile151, Leu161), salt bridges (Asp94-Arg135, Glu97-His160 and an~~
460 ~~aromatic ring sandwich (His160-Trp92-Phe136). Some labels are omitted for clarity. Nitrogen~~
461 ~~atoms are shown in blue and oxygen atoms in red.~~

462

463 **Figure 1 Structure of *E. coli* PBP3.** Cartoon representation of the crystal structure of
464 PBP3$_{57-577}$. A ribbon trace of modelled loops undefined in the crystal structure is shown in
465 grey. The active site is indicated by a red sphere. Loops discussed in the text are indicated.

466

467 **Figure 2 PBP3 active site**. (a) Stereo view of a modelled tripeptide D-Glu-mDap-D-Ala in
468 the active site of PBP3. The tripeptide (yellow) is modelled as an acyl-enzyme and is bonded
469 to the active serine shown in green. (b) Stereo view of a cartoon representation of the

transpeptidase active site of PBP3. The oxyanion hole is defined by the nitrogen atoms of residues 307 and 497. Loop 400-420 is shown in cyan. Nitrogen atoms are shown in blue and oxygen atoms in red.

**Figure 3 Junction between C- and N-terminal modules**. Comparison between the relative orientation of N and C-terminal modules of PBP3 (blue), *S. aureus* PBP2a (magenta) and *S. pneumoniae* PBP2b (green). The C-terminal domain of SaPBP2a and SpnPBP2b are superimposed onto the C-terminal domain of PBP3. SaPBP2a (169-237) and SpnPBP2b (104-197) are equivalent to domain 88-165 of PBP3.

**Figure 4 Domain swapping in PBP3$_{88\text{-}165}$.** (a) PBP3$_{88\text{-}165}$ crystal unit cell (space group P1). The 8 chains are organized by pairs with 18 swapped residues. (b) Interactions between swapped residues from chains D (yellow) and H (green), including the hydrophobic cluster around Ile91 (Leu139, Ile151, Leu161), salt bridges (Asp94-Arg135, Glu97-His160 and an aromatic ring sandwich (His160-Trp92-Phe136). Some labels are omitted for clarity. Nitrogen atoms are shown in blue and oxygen atoms in red.

**Figure 5 PBP3 oligomerization.** (a) Chromatogram of PBP3$_{88\text{-}165}$ gel filtration on a Superdex 75 10/300 GL. The first peak elutes at 12.16 ml and the second at 13.52 ml. Carbonic anhydrase (31 kDa) elutes at 11.05 ml and lysozyme (14kDa) at 15.25 ml (data not shown). The buffer was 0.15 M NaCl and 0.1 M Tris, pH 8 1mM EDTA. (b) Chromatogram of PBP3$_{57\text{-}577}$ gel filtration on a Superdex 200 10/300 GL. The first small peak elutes at 13.3 ml, the second at 14.77 ml. Bovine serum albumin used as a standard elutes at 14.12 ml (molecular mass 67 kDa, data not shown). The masses calculated on the basis of the mass

494 standards are 108.5 kDa for the first peak ($PBP3_{57-577}$ dimer) and 58.5 kDa for the second peak
495 ($PBP3_{57-577}$ monomer). The buffer was 20mM Tris HCl pH 8, 0.5 M NaCl.

496
497 **Figure 6. Interaction with peptidoglycan**. Pulldown of $PBP3_{57-577}$ (up) and $PBP3_{88-165}$
498 (down) with and without peptidoglycan sacculi (+ PG and – PG respectively). S, supernatant,
499 W, washing step, P, pellet.

500

**References**


1. Vollmer W, Blanot D, de Pedro MA (2008) Peptidoglycan structure and architecture. FEMS Microbiol Rev 32: 149-167.
2. Young KD (2003) Bacterial shape. Mol Microbiol 49: 571-580.
3. Spratt BG, Pardee AB (1975) Penicillin-binding proteins and cell shape in E. coli. Nature 254: 516-517.
4. Sauvage E, Kerff F, Terrak M, Ayala JA, Charlier P (2008) The penicillin-binding proteins: structure and role in peptidoglycan biosynthesis. FEMS Microbiol Rev 32: 234-258.
5. Ghuysen JM (1991) Serine beta-lactamases and penicillin-binding proteins. Annu Rev Microbiol 45: 37-67.
6. Macheboeuf P, Contreras-Martel C, Job V, Dideberg O, Dessen A (2006) Penicillin binding proteins: key players in bacterial cell cycle and drug resistance processes. FEMS Microbiol Rev 30: 673-691.
7. Goffin C, Ghuysen JM (1998) Multimodular penicillin-binding proteins: an enigmatic family of orthologs and paralogs. Microbiol Mol Biol Rev 62: 1079-1093.
8. Errington J, Daniel RA, Scheffers DJ (2003) Cytokinesis in bacteria. Microbiol Mol Biol Rev 67: 52-65, table of contents.
9. Margolin W (2005) FtsZ and the division of prokaryotic cells and organelles. Nat Rev Mol Cell Biol 6: 862-871.
10. Aarsman ME, Piette A, Fraipont C, Vinkenvleugel TM, Nguyen-Disteche M, et al. (2005) Maturation of the *Escherichia col*i divisome occurs in two steps. Mol Microbiol 55: 1631-1645.
11. Buddelmeijer N, Beckwith J (2004) A complex of the *Escherichia coli* cell division proteins FtsL, FtsB and FtsQ forms independently of its localization to the septal region. Mol Microbiol 52: 1315-1327.
12. Fraipont C, Alexeeva S, Wolf B, van der Ploeg R, Schloesser M, et al. (2011) The integral membrane FtsW protein and peptidoglycan synthase PBP3 form a subcomplex in Escherichia coli. Microbiology 157: 251-259.
13. Dai K, Xu Y, Lutkenhaus J (1993) Cloning and characterization of ftsN, an essential cell division gene in Escherichia coli isolated as a multicopy suppressor of ftsA12(Ts). J Bacteriol 175: 3790-3797.
14. Gerding MA, Ogata Y, Pecora ND, Niki H, de Boer PA (2007) The trans-envelope Tol-Pal complex is part of the cell division machinery and required for proper outer-membrane invagination during cell constriction in E. coli. Mol Microbiol 63: 1008-1025.
15. Bernhardt TG, de Boer PA (2003) The Escherichia coli amidase AmiC is a periplasmic septal ring component exported via the twin-arginine transport pathway. Mol Microbiol 48: 1171-1182.
16. Typas A, Banzhaf M, van den Berg van Saparoea B, Verheul J, Biboy J, et al. (2010) Regulation of peptidoglycan synthesis by outer-membrane proteins. Cell 143: 1097-1109.
17. Bertsche U, Kast T, Wolf B, Fraipont C, Aarsman ME, et al. (2006) Interaction between two murein (peptidoglycan) synthases, PBP3 and PBP1B, in *Escherichia coli*. Mol Microbiol 61: 675-690.
18. Muller P, Ewers C, Bertsche U, Anstett M, Kallis T, et al. (2007) The essential cell division protein FtsN interacts with the murein (peptidoglycan) synthase PBP1B in Escherichia coli. J Biol Chem 282: 36394-36402.

19. Di Lallo G, Fagioli M, Barionovi D, Ghelardini P, Paolozzi L (2003) Use of a two-hybrid assay to study the assembly of a complex multicomponent protein machinery: bacterial septosome differentiation. Microbiology 149: 3353-3359.
20. Karimova G, Dautin N, Ladant D (2005) Interaction network among *Escherichia coli* membrane proteins involved in cell division as revealed by bacterial two-hybrid analysis. J Bacteriol 187: 2233-2243.
21. Nagasawa H, Sakagami Y, Suzuki A, Suzuki H, Hara H, et al. (1989) Determination of the cleavage site involved in C-terminal processing of penicillin-binding protein 3 of Escherichia coli. J Bacteriol 171: 5890-5893.
22. Miroux B, Walker JE (1996) Over-production of proteins in Escherichia coli: mutant hosts that allow synthesis of some membrane proteins and globular proteins at high levels. J Mol Biol 260: 289-298.
23. Fraipont C, Adam M, Nguyen-Disteche M, Keck W, Van Beeumen J, et al. (1994) Engineering and overexpression of periplasmic forms of the penicillin-binding protein 3 of Escherichia coli. Biochem J 298 ( Pt 1): 189-195.
24. Leslie AGW (1991) Molecular data processing. Crystallographic Computing 5: 50-61.
25. CCP4 (1994) The CCP4 suite: programs for protein crystallography. Acta Crystallogr D Biol Crystallogr 50: 760-763.
26. McCoy AJ, Grosse-Kunstleve RW, Adams PD, Winn MD, Storoni LC, et al. (2007) Phaser crystallographic software. J Appl Crystallogr 40: 658-674.
27. Murshudov GN, Vagin AA, Dodson EJ (1997) Refinement of macromolecular structures by the maximum-likelihood method. Acta Crystallogr D Biol Crystallogr 53: 240-255.
28. Painter J, Merritt EA (2006) Optimal description of a protein structure in terms of multiple groups undergoing TLS motion. Acta Crystallogr D Biol Crystallogr 62: 439-450.
29. Emsley P, Cowtan K (2004) Coot: model-building tools for molecular graphics. Acta Crystallogr D Biol Crystallogr 60: 2126-2132.
30. Kabsch W (2010) Integration, scaling, space-group assignment and post-refinement. Acta Crystallogr D Biol Crystallogr 66: 133-144.
31. Sheldrick GM (2010) Experimental phasing with SHELXC/D/E: combining chain tracing with density modification. Acta Crystallogr D Biol Crystallogr 66: 479-485.
32. Zhang KY, Cowtan K, Main P (1997) Combining constraints for electron-density modification. Methods Enzymol 277: 53-64.
33. Cowtan K (2006) The Buccaneer software for automated model building. 1. Tracing protein chains. Acta Crystallogr D Biol Crystallogr 62: 1002-1011.
34. Garcia De La Torre J, Huertas ML, Carrasco B (2000) Calculation of hydrodynamic properties of globular proteins from their atomic-level structure. Biophys J 78: 719-730.
35. Powell AJ, Tomberg J, Deacon AM, Nicholas RA, Davies C (2009) Crystal structures of penicillin-binding protein 2 from penicillin-susceptible and -resistant strains of Neisseria gonorrhoeae reveal an unexpectedly subtle mechanism for antibiotic resistance. J Biol Chem 284: 1202-1212.
36. Massova I, Mobashery S (1998) Kinship and diversification of bacterial penicillin-binding proteins and beta-lactamases. Antimicrob Agents Chemother 42: 1-17.
37. Han S, Caspers N, Zaniewski RP, Lacey BM, Tomaras AP, et al. (2011) Distinctive attributes of beta-lactam target proteins in Acinetobacter baumannii relevant to development of new antibiotics. J Am Chem Soc 133: 20536-20545.
38. Sainsbury S, Bird L, Rao V, Shepherd SM, Stuart DI, et al. (2011) Crystal structures of penicillin-binding protein 3 from Pseudomonas aeruginosa: comparison of native and antibiotic-bound forms. J Mol Biol 405: 173-184.

598 39. Fedarovich A, Nicholas RA, Davies C (2010) Unusual conformation of the SxN motif in
599 the crystal structure of penicillin-binding protein A from Mycobacterium tuberculosis.
600 J Mol Biol 398: 54-65.
601 40. Pares S, Mouz N, Petillot Y, Hakenbeck R, Dideberg O (1996) X-ray structure of
602 *Streptococcus pneumoniae* PBP2x, a primary penicillin target enzyme. Nat Struct Biol
603 3: 284-289.
604 41. Contreras-Martel C, Dahout-Gonzalez C, Martins Ados S, Kotnik M, Dessen A (2009)
605 PBP active site flexibility as the key mechanism for beta-lactam resistance in
606 pneumococci. J Mol Biol 387: 899-909.
607 42. Lim D, Strynadka NC (2002) Structural basis for the beta lactam resistance of PBP2a
608 from methicillin-resistant *Staphylococcus aureus*. Nat Struct Biol 9: 870-876.
609 43. Nicola G, Peddi S, Stefanova M, Nicholas RA, Gutheil WG, et al. (2005) Crystal structure
610 of *Escherichia coli* penicillin-binding protein 5 bound to a tripeptide boronic acid
611 inhibitor: a role for Ser-110 in deacylation. Biochemistry 44: 8207-8217.
612 44. Dzhekieva L, Rocaboy M, Kerff F, Charlier P, Sauvage E, et al. (2010) Crystal structure
613 of a complex between the Actinomadura R39 DD-peptidase and a peptidoglycan-
614 mimetic boronate inhibitor: interpretation of a transition state analogue in terms of
615 catalytic mechanism. Biochemistry 49: 6411-6419.
616 45. Sauvage E, Duez C, Herman R, Kerff F, Petrella S, et al. (2007) Crystal Structure of the
617 *Bacillus subtilis* Penicillin-binding Protein 4a, and its Complex with a Peptidoglycan
618 Mimetic Peptide. J Mol Biol.
619 46. Taschner PE, Ypenburg N, Spratt BG, Woldringh CL (1988) An amino acid substitution
620 in penicillin-binding protein 3 creates pointed polar caps in Escherichia coli. J
621 Bacteriol 170: 4828-4837.
622 47. Chen Y, Zhang W, Shi Q, Hesek D, Lee M, et al. (2009) Crystal structures of penicillin-
623 binding protein 6 from Escherichia coli. J Am Chem Soc 131: 14345-14354.
624 48. Kishida H, Unzai S, Roper DI, Lloyd A, Park SY, et al. (2006) Crystal structure of
625 penicillin binding protein 4 (dacB) from *Escherichia coli*, both in the native form and
626 covalently linked to various antibiotics. Biochemistry 45: 783-792.
627 49. Sung MT, Lai YT, Huang CY, Chou LY, Shih HW, et al. (2009) Crystal structure of the
628 membrane-bound bifunctional transglycosylase PBP1b from Escherichia coli. Proc
629 Natl Acad Sci U S A 106: 8824-8829.
630 50. Sauvage E, Kerff F, Fonzé E, Herman R, Schoot B, et al. (2002) The 2.4-A crystal
631 structure of the penicillin-resistant penicillin-binding protein PBP5fm from
632 *Enterococcus faecium* in complex with benzylpenicillin. Cell Mol Life Sci 59: 1223-
633 1232.
634 51. Lovering AL, De Castro L, Strynadka NC (2008) Identification of dynamic structural
635 motifs involved in peptidoglycan glycosyltransfer. J Mol Biol 383: 167-177.
636 52. Marrec-Fairley M, Piette A, Gallet X, Brasseur R, Hara H, et al. (2000) Differential
637 functionalities of amphiphilic peptide segments of the cell-septation penicillin-binding
638 protein 3 of *Escherichia coli*. Mol Microbiol 37: 1019-1031.
639 53. Wissel MC, Weiss DS (2004) Genetic analysis of the cell division protein FtsI (PBP3):
640 amino acid substitutions that impair septal localization of FtsI and recruitment of FtsN.
641 J Bacteriol 186: 490-502.
642 54. Sauvage E, Kerff F, Fonze E, Herman R, Schoot B, et al. (2002) The 2.4-A crystal
643 structure of the penicillin-resistant penicillin-binding protein PBP5fm from
644 Enterococcus faecium in complex with benzylpenicillin. Cell Mol Life Sci 59: 1223-
645 1232.

55. Leimanis S, Hoyez N, Hubert S, Laschet M, Sauvage E, et al. (2006) PBP5 complementation of a PBP3 deficiency in *Enterococcus hirae*. J Bacteriol 188: 6298-6307.
56. Yoshida H, Kawai F, Obayashi E, Akashi S, Roper DI, et al. (2012) Crystal Structures of Penicillin-Binding Protein 3 (PBP3) from Methicillin-Resistant Staphylococcus aureus in the Apo and Cefotaxime-Bound Forms. J Mol Biol 423: 351-364.
57. Romeis T, Holtje JV (1994) Specific interaction of penicillin-binding proteins 3 and 7/8 with soluble lytic transglycosylase in *Escherichia coli*. J Biol Chem 269: 21603-21607.
58. Jennings GT, Savino S, Marchetti E, Arico B, Kast T, et al. (2002) GNA33 from Neisseria meningitidis serogroup B encodes a membrane-bound lytic transglycosylase (MltA). Eur J Biochem 269: 3722-3731.
59. Lovell SC, Davis IW, Arendall WB, 3rd, de Bakker PI, Word JM, et al. (2003) Structure validation by Calpha geometry: phi,psi and Cbeta deviation. Proteins 50: 437-450.

671
672 **Table 1:** Data collection and refinement statistics

| Crystal | $PBP3_{57-577}$ | $PBP3_{88-165}$ SeMet derivative | $PBP3_{88-165}$ |
|---|---|---|---|
| PDB code | 4BJP | | 4BJQ |
| Data Collection: | | | |
| Space group | $P6_122$ | P1 | P1 |
| Cell Dimensions | | | |
| a, b, c (Å) | 119.0, 119.0, 139.2 | 55.8, 55.8, 81.5 | 56.0, 56.0, 82.3 |
| α, β, γ (°) | 90, 90, 120 | 75.8, 89.4, 65.3 | 76.2, 89.1, 66.0 |
| Resolution range (Å)[a] | 82.8 – 2.5 (2.64 – 2.5) | 49 – 2.7 (2.85-2.70) | 38.9 - 2.10 (2.21 – 2.10) |
| No. of unique reflections | 20753 | 45763 | 45669 |
| Rmerge (%)[a] | 16.6 (54.3) | 11.7 (47.8) | 8.0 (50.8) |
| <I>/<σI> [a] | 13.5 (4.9) | 8.7 (2.6) | 10.2 (2.5) |
| Completeness (%)[a] | 99.8 (98.8) | 95.4 (93.8) | 88.5 (95.4) |
| Redundancy [a] | 14.0 (10.4) | 2.6 (2.6) | 3.7 (3.8) |
| Refinement: | | | |
| Resolution range (Å) | 59.5 - 2.5 | | 35.7 – 2.1 |
| No. of non hydrogen atoms | 3409 | | 5467 |
| Number of water molecules | 135 | | 533 |
| R cryst (%) | 19.9 | | 20.8 |
| R free (%) | 24.5 | | 26.2 |

| | | | |
|---|---|---|---|
| RMS deviations from ideal Stereochemistry | | | |
| Bond lengths (Å) | 0.012 | | 0.010 |
| Bond angles ($^{o}$) | 1.41 | | 1.19 |
| Mean B factor (all atoms) ($Å^2$) | 34.1 | | 31.9 |
| Ramachandran plot [b] | | | |
| Favoured region (%) | 98.5 | | 99.7 |
| Allowed regions (%) | 1.5 | | 0.3 |
| Outlier regions (%) | 0 | | 0 |

673
674 [a] Statistics for the highest resolution shell are given in parentheses.

675 [b] Using program rampage [59]

676

677

678

**Dear Editors,**

**We have tried to address the concerns of reviewer 1 about the structure. Typographical errors found mainly by reviewer 2 have been corrected and the paper was read by an English native speaker. Finally, as suggested by reviewer 3, we have expanded the description of the structure and modified the figures accordingly. Details follow.**

Reviewer #1

1. lines 125-129 … The authors state that PBP3(57-577) crystalization "could not be reproduced despite countless attempts." First, surely there were not "countless" attempts. About how many attempts were made, and do the authors have any ideas about what the problem might be? This is rather important since it is unlikely that the work can be replicated by others if it cannot be replicated here. Second, with only one successful crystallization, how confident are the authors about the nature of the results?
   **R: The apparent very narrow range of crystallization conditions resulted in only some very small badly diffracting crystals and one crystal diffracting at 2.5 Å. This sentence was added to the manuscript.**
   **In the case of several PBPs structures, the difficulties encountered in obtaining high resolution x-ray data sets, in reproducing crystals or even obtaining crystals, are mainly due to their nature of multi-domain proteins, for which several relative conformations of the different domains co-exist in solution. That's why multi-domain protein structures are frequently determined from a single X-ray dataset but this has no impact on the soundness of structure determination.**

   2. lines 212-213 … The PBP3 structure was evidently not determined de novo, but by comparison with the structure of PBP2 from a different organism, N. gonorrhoeae. This, when combined with the fact that only one crystallization attempt was successful, makes me wonder if this is the real structure of PBP3 or if it is only a single possible structure that can be made to conform to the structure of a somewhat distant homologue. Why can the structure not be generated on its own, and what are the limitations imposed by the modeling method?
   **R: Structure determination by molecular replacement using the structure of a homologous protein (NgPBP2) is also a standard method that does not impact the confidence that the structure determined corresponds to the protein that has been crystallized. R and Rfree values are good criteria to ensure that the structure corresponds to the X-ray measures, independently of the initial structure used for molecular replacement.**
   **Efforts have been made to clearly show in figure 1 the part of the structure that was determined from X-ray data and the modeled parts of the structure.**

   3. lines 378-380 … The authors could not reproduce interactions between the PBP3(88-165) fragment and other cell division proteins. If these interactions do not occur, doesn't this call into question the biological relevance of the structure obtained for this fragment?

**R: No. The structure of the domain 88-165 compares well with the equivalent domains of other class B-PBPs. The biological relevance of the swapping associated with the structure of the domain alone is indeed questionable but we think that the discussion states it clearly.**

4. In Figure S3, very little of the PBP3(57-577) seems to have co-precipitated with the peptidoglycan preparation. Why? The authors should quantify how much was precipitated and compare it to what might be expected.

**R: A similar test was done with LpoA-LpoB (Typas et al, Cell. 2010, 143:1097) without quantification, which is difficult. Clearly, only a fraction of the protein was precipitated. A possible explanation is that PBP3 interacts only with the septal peptidoglycan, which represents only a small proportion of the total peptidoglycan.**

Minor comments

5. line 69 … should be “LpoB” (capital “B”)
**Done**

6. line 256 … should be “PBP-structures” (plural)
**OK**

Reviewer #2

1. There are many typos and errors in comma usage and grammar that should be corrected.

Minor points:

1. l. 47: it is not clear what is meant by "direct" peptidoglycan synthesis. Is there something like indirect synthesis?
**“Direct” has been removed**

2. l. 69: should be "LpoB" with capital "B"
**Done**

3. l. 96: the 2XYT medium should be defined.
**Done**

4. l. 98: should be "0.5 mM"
**Done**

5. l. 113/117/119: what is meant with "ch/h" and "cm/h". Flow rates should be given in "ml/min" or "ml/h".
**R: Typing error, ch/h doesn’t exist, it’s cm/h (linear flow rate, which is independent of the**

**diameter of the column, instead of the flow rate in ml/h which is dependent of the column diameter). The linear flow rate is preferred by people making a scale-up because it's the real value independent of the column size allowing to compare different size of columns; for example 100 mL/h used for two columns having a surface doubling will make a factor two for the residence time.**
**Linear flow rate (cm/h) X surface ($cm^2$) = volumetric flow rate (ml/h)**
**In our case with the XK50 column (diameter = 5 cm surface = 19.63 $cm^2$**
**31 cm/h = 608 mL/h; 15 cm/h = 294 mL/h**

6. l. 122: it is not clear what is meant by "three-dimensional environment with 30% of alpha-helix". Please re-phrase to make the sentence clear.
**R: The sentence was changed.**

7. l. 127: "CAPS" needs to be defined.
**Done**

8. l. 197-202. "KDa" should be corrected to "kDa".
**Done; also in figure legends.**

9. l. 213: missing blank.
**Added**

10. l. 229: define "mDAP"
**Done**

11. l. 264-264: What is meant by "...and the conformation of the segment 402-420 are conserved in all PBPs."? What is meant here with "conformation"? Also, you need to clarify if the "conformation" is conserved in all known PBP structures, or in all class B PBPs, or what is meant here.
**R: The sentence was modified**

12. l. 284. Here, it does not become clear why the comparison with other PBPs provides evidence for flexible junction between the modules. What is the evidence, and how has it been obtained? Also, have other computational methods been used to assess the flexibility?
**R: Evidence is suggested also by apo and acyl structures of PBP3 from Pseudomonas aeruginosa (Sainsbury, JMB, 405, 173-184). The flexibility of the junction also exists in class A PBPs. We have modified the sentence, added a figure as suggested by reviewer 3 remark 9, and added references.**

13. l. 287: what is meant with "processive displacement of the divisome"?
**R: It means divisome displacement during processive glycan chain synthesis. The sentence has been simplified**

14. l. 298: should be "Marrec-Farley" with capitol "F".
**OK (Marrec-Fairley)**

15. l. 425. It must be clearly stated in the heading of the legend and in part (a) that the figure shows a model of the PBP3 structure, and not the crystal structure itself (as is written).
**R: The figure was modified according to reviewer3's suggestion showing now the crystal structure in cartoon and a light trace of the modelled loops.**

16. l. 431. should be "Tyr".
**OK**

17. Figure 1: should it be "Loop 202-228" (instead of "Loop 220-228") to be consistent with the text?
**R: The correction was done in figure 1**

Reviewer #3:
1. Analysis of Figure 1 gives the reader the impression that the structure includes the transmembrane region, as well as the full N-terminal domain. Reading of the figure legend, however, indicates that the TM was modeled, and so were all of the regions in cyan. Since this is a very important figure for the paper, and could be eventually used by other scientists for teaching, etc, it should only include the regions that could be traced in a trustworthy fashion in the map. The TM region does not have to be included (it is not helpful for the figure, or even mentioned in the text), and all loops and regions that were modeled should be replaced by dots.

**R: The figure has been modified as suggested by the reviewer. The modeled loops are now shown in very light grey and the TM helix has been removed. We have also followed the reviewer's remark 15 suggesting showing beta-strands colored differently from alpha-helices.**

2. It is unclear to the reader why authors started their clone at residue 57; a schematic figure could be included, describing the exact construct that was used and the structure that was traced.

**R: The construct starting at residue 57 was less prone to degradation that a construct starting at residue 37. See Fraipont C et al. (1994) Engineering and overexpression of periplasmic forms of the penicillin-binding protein 3 of Escherichia coli. Biochem J 298 ( Pt 1): 189-195. The reference has been added in the material and method section.**

**Figure 1 now clearly shows the construct and the difference between what was seen in the map and the modeled loops.**

3. P. 10, lines 220-221, it is rather strange to mention that the C-terminus is associated to the N-terminus; do authors mean to say that it interacts closely?

**R: The sentence has been made clearer.**

4. Although one has the impression that there are 4 individual figures, in fact they are only 2, parts A and B of the same figure having been separated into different files. As a consequence, this manuscript only has 2 figures. Authors could illustrate their manuscript better by adding additional figures; for example, showing the 'long groove' that is alluded to on p. 10, lines 227-228.

**R: We have added some figures: a model with part of the substrate showing the long groove (remark 5) and a figure showing the superposition of different class B-PBPs (remark 9). We have included the supplementary figures in the manuscript.**

**Figure 1: structure of PBP3**

**Figure 2: Active site**

**Figure 3: Junction**

**Figure 4: Domain 88-165**

**Figure 5 : PBP3 oligomerization**

**Figure 6 : Interaction with peptidoglycan**

5. There is a paper from the Mobashery lab describing the structure of an E. coli PBP (5/6) with a peptide in the active site; since authors mention that their long groove could bind substrate, how does it compare to this paper? Is it possible to model a peptide in their structure?

**R: We have modeled the acyl-enzyme with D-Glu-mDap-D-Ala linked to the active serine and made a figure of it. The model is based on an unpublished acyl-enzyme structure that we have obtained with another PBP (the DD-peptidase from Actinomadura R39) rather than the Mobashery's one, which has a lysine instead of diaminopimelic acid in the peptide**

6. P.10, after lines 223-224, a reference should be cited.

**R: As lines 223-224 are empty, we believe that reviewer's remark relates to lines 233-234, where we have added a reference.**

7. P.12, this part of the text refers to figure 1b, which is rather problematic. Details about a pocket are described, but by looking at the figure one does not have the impression to see a pocket; since one of the beta-strands was shown as sticks (which is not really helpful), it gives the reader the impression that there is a peptide bound to the active site. In order to make this clearer, authors should show the active site with arrows for beta strands (that should be labeled as per other PBPs … the beta-strands neighboring the active site on this figure are beta3 and beta4).

**R: There are now two figures showing the active site. The first (figure 2a) shows the groove (cf remark 5) and the second is the former figure 1b (now 2b) modified as suggested by the reviewer (strand beta3 shown as a strand and labeled). Both are in stereo (cf remark 13)**

8. P.12, lines 269-270: please mention the nomenclature for the beta strands involved, and add references here.

**R: Nomenclature and references have been added**

9. P.12, lines 283-284: these interesting sentences could be illustrated by a figure highlighting the differences between junctions for different PBPs (and references should also be added)

**R: Details were added to the text and a new figure illustrates these sentences (figure 3).**

10. 9. P. 14, line 310, please replace 'tridimensional' by 'three-dimensional'

**Done**

11. If authors only have 2 figures in their manuscript, why did they include three supplementary figures? All of the data can be included in the main text.

**We have integrated all the figures in the manuscript**

12. It is curious that on p. 16 lines 374-375 authors discuss the fact that a role for domain swapping in the in vivo dimerization process of PBP3 is elusive, and in lines 380-381 go on to discuss that their could be a role for this in vivo.

**R: In lines 380-381, we mention the possible influence of the in vitro dimerization of domain 88-165 on the result of interaction tests. We have slightly modified the sentence to avoid confusion**

13. Figure 1, legend: this reviewer recommends that secondary strand elements be labeled, as suggested above. What do authors mean by 'unhide' Tyr514? If their objective is to show it clearly, they could potentially change the angle, or make a stereo figure, or make a LigPlot figure ...

**R: See remark 7**

14. I'm not quite sure how relevant Fig. 2b is, especially considering that authors clearly mention that these interactions are probably not relevant in the full-length PBP3 structure. They could potentially replace it by supplementary data, or other images of the full-length crystal structure. What does a surface charge diagram look like?

**R: We have kept this illustration, which makes the description of the swapping easier to understand.**

15. These authors published a beautiful review article in FEMS a few years ago where they showed the transpeptidase domain of PBPs with beta-strands colored differently from alpha-helices; they could perhaps adopt that strategy for this paper, and modify Figs. 1a/1b accordingly.

**R: We have modified figure 1 as suggested**